AN ABSTRACT OF THE THESIS OF

Ida M. Royer for the degree of Master of Science in Oceanography presented on June 2, 2008.

Title: An Investigation into Nitrogen Uptake by *Emiliania huxleyi* during Continuous Darkness.

Abstract approved:

_____

Fredrick G. Prahl

Experiments were conducted with two strains of the coccolithophorid *Emiliania huxleyi*. Previous experiments with CCMP1742 and 372 at a light intensity of 60 μEin/m^2-s showed that during five-day periods of continuous darkness, strain 1742 was taking up nitrate from the media while strain 372 was not. The nitrate uptake in strain 1742 was concurrent with an increase in particulate nitrogen. This observation, combined with the fact that carbon-rich alkenones decreased during the same dark period, led to the hypothesis that amino acids were being synthesized during the continuous darkness period in *E. huxleyi* strain 1742.

This thesis presents results from three separate continuous darkness experiments with *E. huxleyi* strains 1742 and 372, run at a light intensity of 165 μEin/m^2-s. These experiments were conducted to determine whether 1) amino acids are synthesized in *E. huxleyi* strain 1742 during continuous darkness, 2) this strain is physiologically unique in this regard, and 3) any amino acid accumulation is compound-specific. Two separate and independent methods for amino acid determination were utilized: gas chromatography

paired with a flame ionization detector (GC-FID) and the ninhydrin method. Alkenones, media nutrients, and particulate organic carbon and particulate nitrogen (PN) were also measured.

Results showed that no dark-period nutrient uptake or PN accumulation occurred in strain 372, in agreement with previous findings. No accumulation of amino acids was displayed in this strain during the continuous darkness period. CCMP1742 displayed nitrogen uptake, PN accumulation, and amino acid synthesis during the first experiment, but not the second or third experiments. The argument is presented that the increased light intensity of 165 $\mu Ein/m^2$-s inhibited the above dark-period nitrogen dynamics. This inhibition may have been overcome in the first experiment due to a previous nutrient stress experienced by the cells used to inoculate the experiment culture. Future experiments should utilize $^{15}NO_3$ to track the media nitrogen into cells, and also investigate the effects of light intensity and nutrient stress on dark-period protein production.

An Investigation into Nitrogen Uptake by *Emilania huxleyi* during Continuous Darkness

by
Ida M. Royer

A THESIS

submitted to

Oregon State University

in partial fulfillment of
the requirements for the
degree of

Master of Science

Presented June 2, 2008
Commencement June 2009

Master of Science thesis of Ida M. Royer presented on June 2, 2008.

APPROVED:

Major Professor, representing Oceanography

Dean of College of Oceanic and Atmospheric Sciences

Dean of the Graduate School

I understand that my thesis will become part of the permanent collection of Oregon State University libraries. My signature below authorizes release of my thesis to any reader upon request.

Ida M. Royer, author

ACKNOWLEDGEMENTS

I thank:

Dr. Fred Prahl (NSF grant OCE-9986306, Oregon Space Grant), for investing in me and not giving up on me. For always making time, keeping me on target, and asking what I'm up to. For the awesome field experience and enthusiasm.

Dr. Pat Wheeler and Dr. Vincent Remcho, for serving the important and time-consuming role of committee members, and to Dr. Michael Lerner for being my graduate representative.

Margaret Sparrow, for always answering my dumb questions with a straight face and the many, many hours of help. The lab is a happier place when you're in it.

Amanda Ashe, for growing the non-Ehux phytoplankton cultures used in this work, making the related Coulter Counter measurements, and being so great about it.

Laure Brooks and Cooper, Danny, and Rob for the support, love, and encouragement that pushed me to the finish line.

My dad and sister, for the steady and constant love that makes you sleep better.

Russ, for putting a roof over my head. Thank you thank you! Also for the great chocolate and music trivia.

Dr. Tim Cowles, for giving me an opportunity to tour the optical and acoustical side. And Mike Wetz, for taking time to read my thesis.

The friends who've made life sunnier. Zach and Jess and Becky. The various people I've bumped into along the way.

Myself, for being an incredible, strong, and beautiful woman.

TABLE OF CONTENTS

TABLE OF CONTENTS (Continued)

LIST OF FIGURES

LIST OF TABLES

LIST OF APPENDIX TABLES

An investigation into nitrogen uptake by *Emiliania huxleyi* during continuous darkness

Introduction

Oceanographers researching historic and present-day global climate are interested in the coccolithophore *Emiliania huxleyi* for a number of reasons. It produces dimethylsulfoniopropionate (DMSP), a precursor of dimethylsulfide (DMS), which can ultimately play a role in cloud formation (Vallina et al., 2007). It calcifies, at times so copiously the water turns a milky white visible from space (Holligan et al., 1993). Calcification produces carbon dioxide as a by-product and counteracts the photosynthetic benefits of plant growth on carbon dioxide drawdown (Frankignoulle et al., 1994). In addition, *E. huxleyi* makes unusual lipid biomarkers—alkenones—which survive burial in the sedimentary record. The unsaturation patterns in these compounds change with the growth temperature of the organism. Hence, alkenones are now widely used as a promising paleo-proxy for mean annual sea surface temperature (maSST) (Herbert, 2003).

Muller et al. (1998) collected alkenone data (60^{o}N to 60^{o}S) from marine surface sediments. Figure 1.1 (annotated by Prahl et al., 2003) plots the unsaturation patterns of the alkenones, denoted $U_{37}^{K'}$, versus the maSST of the overlying waters. The trend is distinct, with a dashed line representing the best fit ("global average"; $U_{37}^{K'} = 0.033\text{T} + 0.069$). Overlying this dashed line is a solid one calculated from batch culture experiments with *E. huxleyi* strain 1742 (Prahl et al., 1988; $U_{37}^{K'} = 0.034\text{T} + 0.039$).

Remarkably, the field data and laboratory data for this specific stain of *E. huxleyi* are statistically similar (Muller et al., 1998).

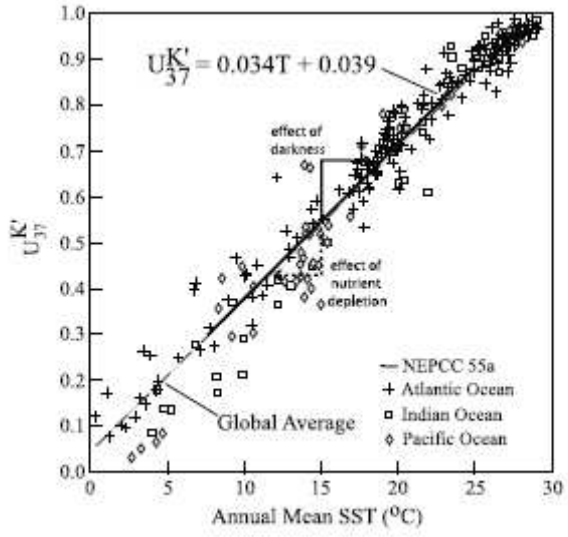

Figure 1.1: Global alkenone data taken from sediment core tops (Muller et al., 1998). Alkenone unsaturation patterns ($U^{K'}_{37}$) are plotted versus the mean annual SST of the overlying waters. The best fit line through these data (Global Average) closely matches the laboratory calibration for *E. huxleyi* strain 1742. Under isothermal conditions, the stress of nutrient depletion (dashed line) causes a decrease in $U^{K'}_{37}$ (~0.014) in strain 1742 that equates to a ~3°C underestimation using the calibration. Under the same isothermal conditions, continuous darkness (solid line) causes a comparable overestimation of $U^{K'}_{37}$, and consequently temperature (~ 3°C). (Taken from Prahl et al., 2003.)

Despite the promise shown by this work, the use of alkenones as a paleo-proxy contains uncertainties which stem from an incomplete knowledge of *E. huxleyi*'s biochemistry and physiology. Though *E. huxleyi* is a major alkenone-producer and, in general, its $U^{K'}_{37}$-growth temperature calibration curve matches the global $U^{K'}_{37}$-mean annual SST calibration, this organism is not the only haptophyte capable of alkenone production (Marlowe et al., 1984), and the other source organisms do not all

biosynthesize alkenones identically (Conte et al., 1998). In addition, isothermal culture experiments with *E. huxleyi* strain 1742 have shown that, aside from temperature, both stresses from nutrient depletion and exposure to darkness can affect $U_{37}^{K'}$ (Prahl et al., 2003). Prahl et al. (2003) superimposed this stress-induced variability in $U_{37}^{K'}$ on the global coretop calibration (Fig. 1.1) and showed it corresponds to a temperature error of ± 3^{o}C. Much of the scatter in the field data from Muller et al. (1998) could potentially be explained by nonthermal physiological factors which operate in natural environments.

Studies were conducted to elucidate the non-thermal impacts on alkenone production ($U_{37}^{K'}$), revealing some curious observations. Isothermal, exponentially-growing batch cultures with *E. huxleyi* strain 1742 were placed under nutrient replete conditions in continuous darkness for five days. Though cell growth was suspended, drawdown of both nitrate and phosphate occurred in the media (figures 1.2a and b). The decrease in the nitrate content of the media was matched with a nearly stoichiometric increase in particulate nitrogen (PN) (figure 1.2c) with no accompanying particulate organic carbon (POC) decrease (figure 1.2c), despite the loss of carbon-rich alkenones (figure 1.2d). The apparent loss of alkenones was equivalent to 24 μM C or ~15% of the POC signal. Interestingly, the molar ratio of alkenone carbon loss to PN gain was ~2, versus ~3.5 for average amino acids (Hedges et al., 2002). This observation leads to the first question that will be addressed in this thesis:

Q1 - Are *E. huxleyi* cells manufacturing amino acids in prolonged darkness using media nitrate and cellular alkenone carbon?

Preliminary studies have also revealed that these curious observations of a strain of *E. huxleyi* isolated from the subarctic Pacific (CCMP1742) are not common to all strains of this organism available in culture collections. Results from virtually identical batch culture experiments conducted with a strain from the Sargasso Sea (CCMP372, figure 1.3) and from a Norwegian fjord (CCMP370) (Appendix A) showed no gain of PN in darkness. In addition, the alkenone loss in these strains was far less significant during the dark period and more abrupt, with the loss complete by the second day rather than a gradual decrease over the entire dark period as observed in strain 1742. These findings lead to the second question to be addressed in this thesis:

Q2 - Is CCMP1742 a physiologically unique strain of *E. huxleyi* with respect to cellular nitrogen dynamics?

In order to best answer the two questions posed above, a suitable method for quantitative amino acid analysis had to be adopted. For this purpose, capillary gas chromatography with flame ionization detection (GC-FID) was pursued as a method of choice. The GC-FID method allows not only a way to quantify the total amino acid content of cells as a function of growth condition (i.e., exponentially dividing versus darkness-imposed stationary phase) but also the molecular composition of the amino acid mixture. The latter attribute of the method allowed the third and final question to be addressed in this thesis:

Q3 - If amino acids are biosynthesized in prolonged darkness by certain strains of *E. huxleyi*, is biosynthesis compound specific?

Figure 1.2: Data for a batch culture, continuous darkness experiment with *E. huxleyi* strain 1742 (60 μEin/m^2s, ~15^{o}C, f/20 media) in November 2001 (Prahl and coworkers, unpublished data; see Appendix A). Boxed areas represent a period of continuous darkness, otherwise cells were on a diel (12:12) light cycle. Though cell growth was suspended during continuous darkness (a), nitrate and phosphate drawdown occurred (b) with a nitrate to orthophosphate ratio averaging ~15:1, close to Redfield stoichiometry. Nitrate decreased by 19 μM during the dark period (b) while simultaneously PN increased by 14 μM (c), pointing to a movement of nitrogen from the media into cells. POC did not decrease despite a loss of alkenones equating to 24 μM carbon (d), or ~15% of the dark-period POC, suggesting that the alkenone carbon was used to form a different cellular constituent and not merely lost as a respiration product.

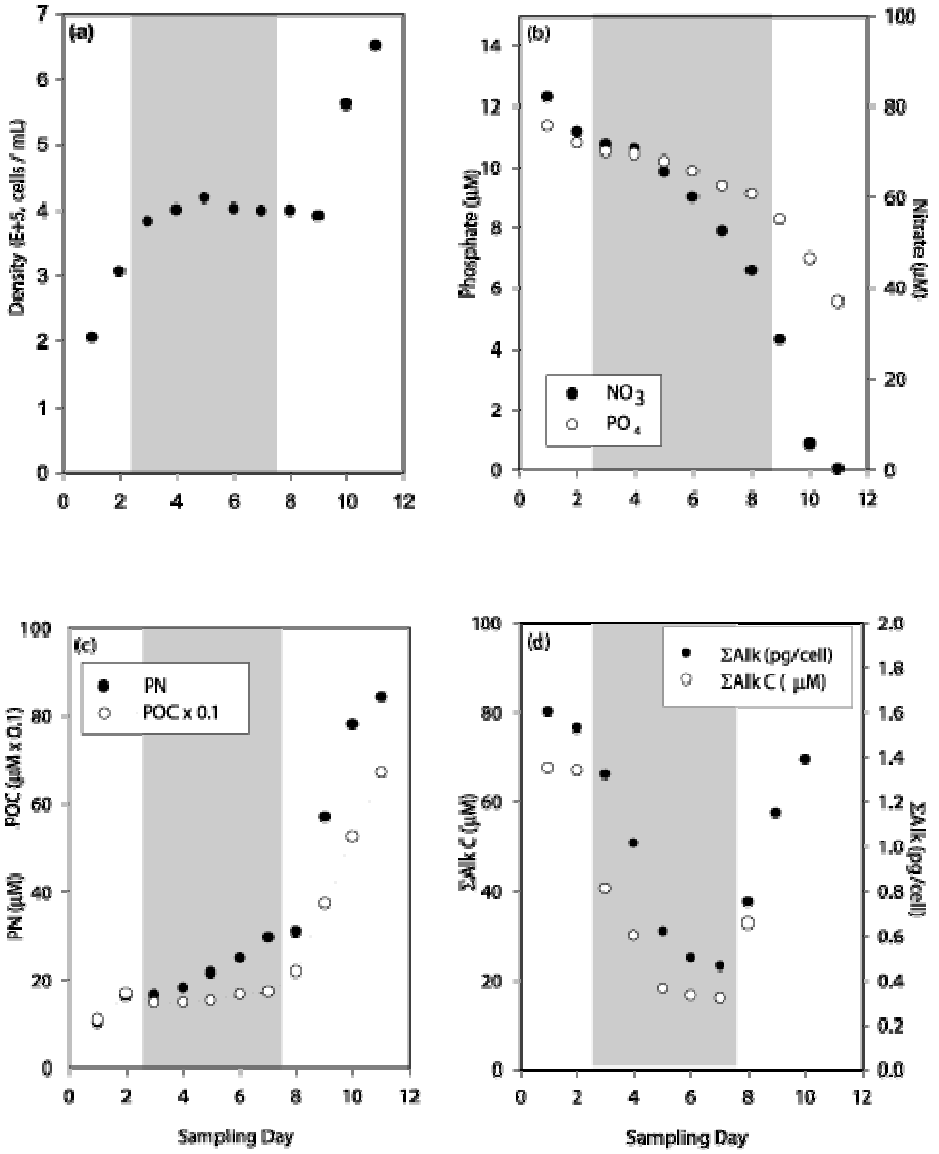
(a)
Density (E+5, cells / mL)
(b)
Phosphate (µM)
Nitrate (µM)
NO3
PO4
(c)
PN
POC x 0.1
POC (µM x 0.1)
PN (µM)
Sampling Day
(d)
ΣAlk (pg/cell)
ΣAlk C (µM)
ΣAlk C (µM)
ΣAlk (pg/cell)
Sampling Day

Figure 1.2

Figure 1.3: Data for a batch culture, continuous darkness experiment with *E. huxleyi* strain 372, in October 2002 (Prahl and coworkers, unpublished data; see Appendix A), with identical parameters as figure 1.2. During continuous darkness (boxed areas) cell growth was suspended (a), as in strain 1742. However, strain 372 experienced no nitrate or phosphate drawdown in the media (b) and PN remained unchanged during the dark (c), averaging 19 ± 1.4 μM. POC did not decrease during continuous darkness (c), averaging 140 μM. Though dark-period alkenone levels decreased overall by 5 μM of carbon (d), or ~5% of the dark-period POC, the loss was much less than that for strain 1742.

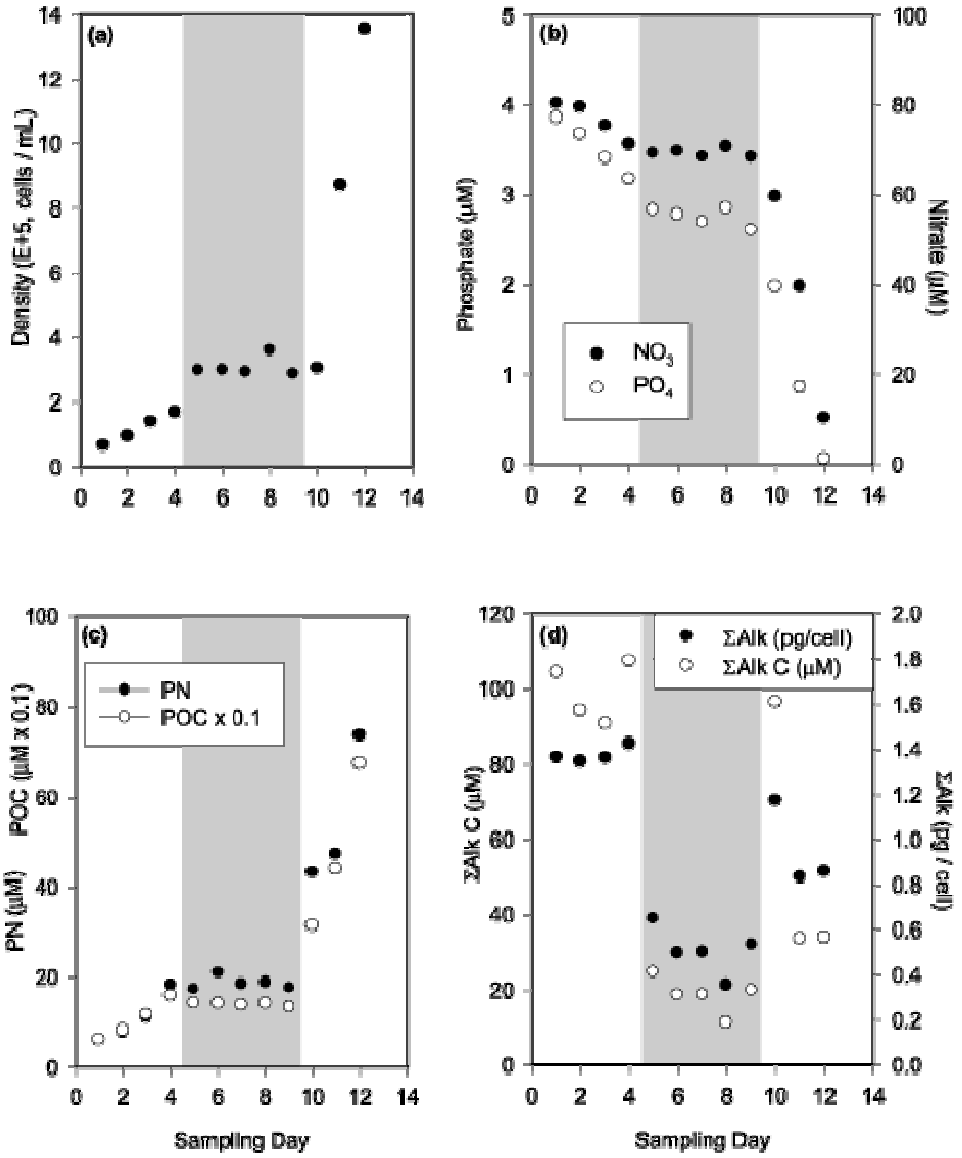
(a)
Density (E+5, cells / mL)
(b)
Phosphate (µM)
Nitrate (µM)
NO3
PO4
(c)
PN
POC x 0.1
PN (µM)
POC (µM x 0.1)
Sampling Day
(d)
ΣAlk (pg/cell)
ΣAlk C (µM)
ΣAlk C (µM)
ΣAlk (pg / cell)
Sampling Day

Figure 1.3

Methods

2.1 Cultures

Two strains of *E. huxleyi*, obtained from the Provasoli-Guillard National Center for Culture of Marine Phytoplankton (CCMP), were compared. Strain 372 was originally isolated from near the BATS station in the Sargasso Sea, located in a subtropical gyre where winter mixing occurs along with potential nitrogen fixation (Lipschultz et al., 2002). Strain 1742 was isolated from station 'P' in the subarctic pacific, a high-nutrient, low-chlorophyll region in which plant stock levels remain low year-round (Cooney, 2004). Both strains were maintained in the laboratory as batch cultures, and no longer calcify.

Cultures were grown in sterilized Erlenmeyer flasks (125 mL) containing 75 mL of f/20 media (http://ccmp.bigelow.org/CI/CI01e.html), which were fitted with cotton-stuffed cheesecloth stoppers and covered with an upside-down beaker to prevent biological contamination. Transfers occurred every two weeks in a laminar flow clean hood using autoclaved glassware, stoppers, and media. The cultures were maintained at 15^{o}C and at a light intensity of 165 μEin/m^{2}-s, over twice that used in the previous experiments (Figs. 1.1 and 1.2), using cool white fluorescent lights set on a 12:12 diel light cycle.

In the three sets of experiments conducted for this study, batch cultures were grown identically as the maintained cultures, but in 1 L Erlenmeyer flasks containing 800 mL of the f/20 media. At a mid-exponential stage of growth, cells of a given strain were placed in continuous darkness for five days to examine the effect on nitrogen uptake. For

each experiment, flasks were inoculated with cells taken from the non-axenic stock cultures, one with strain 1742 and one with strain 372, with the transfer procedure described above. These experimental flasks were placed in a temperature-controlled water bath set to 14^{o}C, which was monitored using a Hobo logging thermistor (http://www.onsetcomp.com). A bank of cool white fluorescent lights sat below and to one side of the tank, yielding an illumination of ~165 μEin/m^2-s in each flask.

Samples for both cell counts and biochemical analyses were collected during the experiments. Samples were collected in the walk-in cooler to prevent undue stress on the cells in culture, and were taken at the same time each day to minimize any biochemical changes related to diel division cycles. Flasks were swirled prior to sampling to ensure a representative sample. Care was also taken to minimize free-air exposure.

Cell counts were made every day of the experiment, using a small volume (less than 1 mL) of culture, a hemocytometer, and a Heerbrugg WILD light microscope (12.5x magnification) (Fig 2.1). Once the cultures reached the midpoint of exponential growth (~250,000 cells/mL, based on previous experiments), the experimental flasks were wrapped completely with aluminum foil to impose total darkness on cells while leaving all other growth conditions unchanged. After a five day period, the foil was removed and the cells were again exposed to the original diel light cycle.

Sampling for biochemical analysis focused on the period of darkness. As shown in Fig. 2.1, sampling was done each day beginning two days before and extending until two days after the period of continuous darkness. The total culture volume required for sampling each day (75 mL) was taken all at once and covered between the various chemical processing steps, which were completed within two hours. During the nine-day

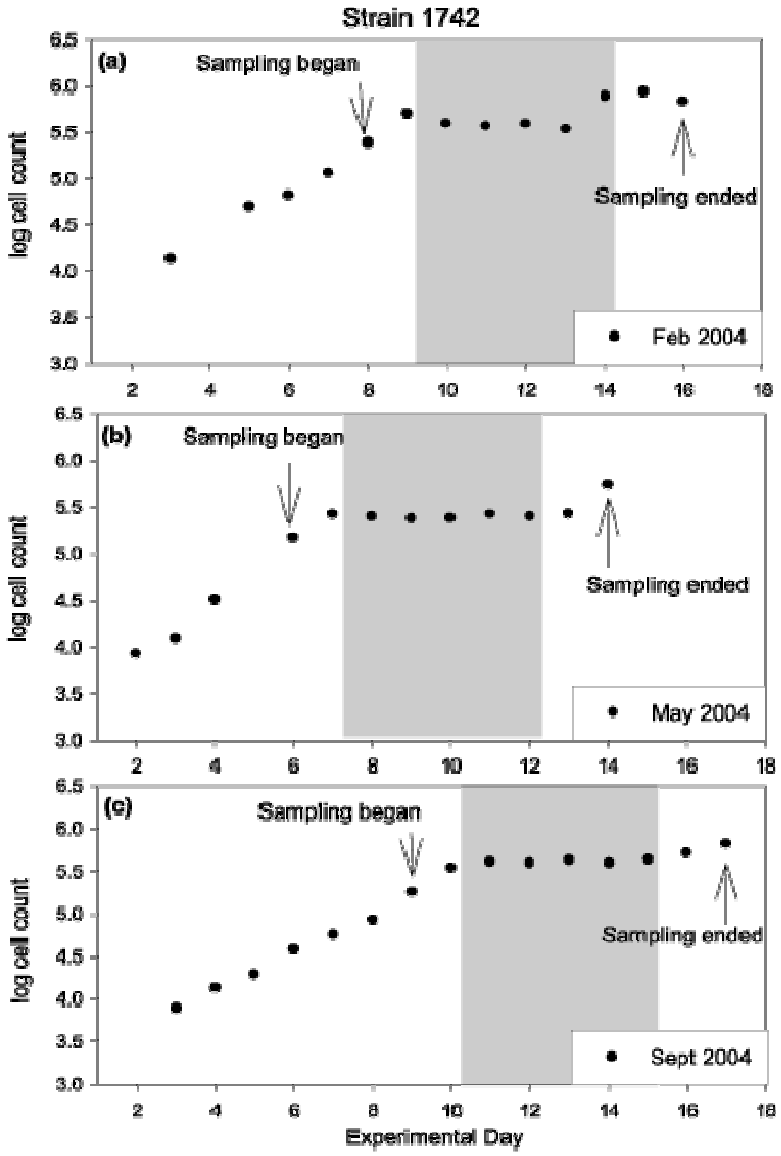

Figure 2.1: Growth curves for the February (a), May (b), and September (c) experiments with strain 1742, and for the May (d) and September (e) experiments with strain 372. Boxed areas are periods during which cells were placed iinto complete, continuous darkness, otherwise cells were on a 12:12 diel light cycle. Sampling began two days before continuous darkness and ended two days after.

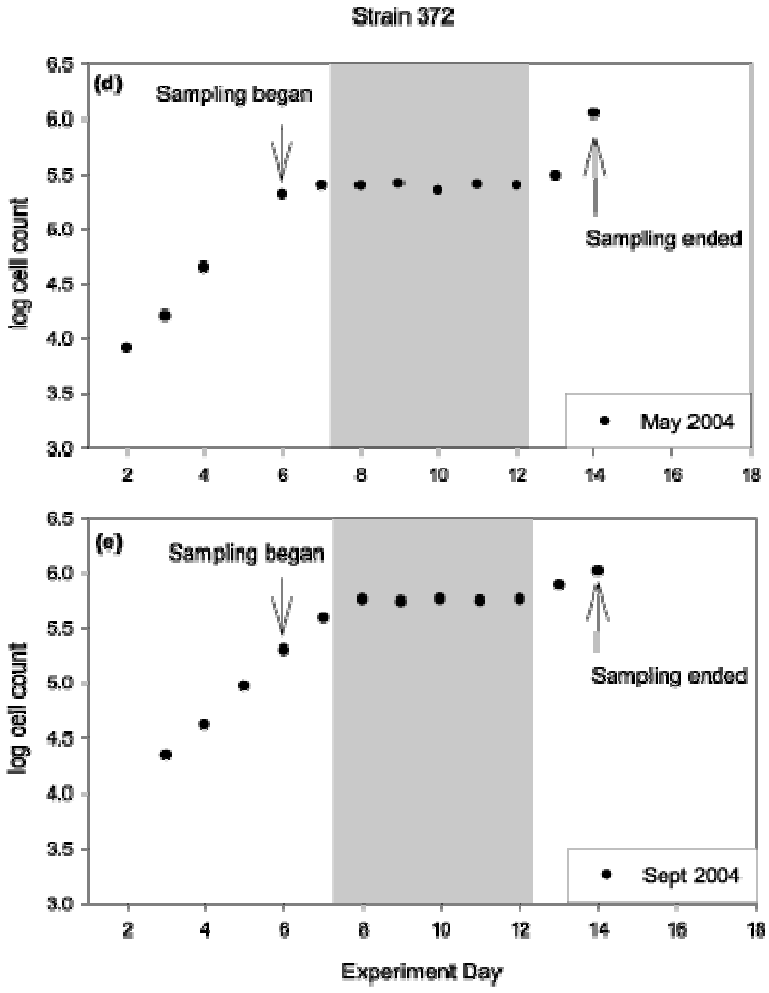

Figure 2.1 (continued)

period of chemical sampling, cell counts were determined from this volume. By the end of the experiment, less than 200 mL of culture remained in the experimental flask.

2.2 Filtration

E. huxleyi cells were isolated from the culture media via gentle vacuum filtration. Samples were isolated for alkenones (~10 mL), particulate organic carbon and nitrogen (POC/PN, ~20 mL) and total hydrolysable amino acids (THAA) via both spectrophotometry (~20-25 mL) and gas chromatography with flame ionization detection (GC-FID, ~20-25 mL). Cells for alkenone and POC/PN analysis were collected on pre-combusted (450^{o}C, 4 hrs) glass fiber (Whatman GF/F) filters (25 mm). Preliminary analysis of amino acids via GC-FID showed that water adsorption onto GF/F filters prevented quantitative derivitization of amino acids. Therefore, polycarbonate membrane filters (Nuclepore, 25 mm, 0.2-0.4 μm) were used for all amino acid analyses. All filters were folded, wrapped in aluminum foil, and stored at -80^{o}C until analysis. Filtrate was collected (~30 mL) for nutrient analysis (total nitrate plus nitrite or N+N, nitrite, and phosphate), stored frozen in a standard chest freezer, and analyzed via an autoanalyzer by an outside laboratory using well established methods (Strickland and Parson, 1972).

2.3. Amino Acid Determination

In order to quantify the total amino acid (THAA) content of *E. huxleyi* cells, cellular proteins were first hydrolyzed into individual amino acid constituents using the method of Cowie and Hedges (1992). Briefly, *E. huxleyi* cells on the membrane filters were each placed in a 1 mL reaction vial and 0.8 to 1 mL of 6 N HCl was added. The

vials were sealed with teflon-lined caps and heated at 150^{o}C for 1 hour. Once cooled, the hydrolysate was then transferred to a new reaction vial and the empty, filter-containing vials were rinsed (3x, 1 mL) with acid (6 N HCl). The rinses were combined with the original hydrolysate and the acidic solution was then evaporated to dryness under a stream of pre-purified N_2.

Samples for the protein standard bovine serum albumin (BSA, see section 3.1) were likewise dissolved in 6 N HCl (~1 mL) prior to hydrolysis as described above.

2.3.1 *GC-FID method*

Amino acid samples for gas chromatographic – flame ionization detection (GC-FID) analysis were spiked with two internal standards during the hydrolysis procedure. A dilute solution of norvaline (0.005 M dissolved in 0.1 N HCl, 50 μL), was added to the vials just prior to the final N_2 evaporation step. A second internal standard, α-amino-n-butyric acid (0.005 M dissolved in 0.1 N HCl, 50 μL) was added to the hydrolysate prior to the vial transfer and rinses. Use of α-amino-n-butyric acid as a recovery standard was found to generate more erratic amino acid values, and hence norvaline was the default internal standard in all samples.

Derivitization: Total hydrolyzed amino acids (THAA) were converted to their propyl ester, trifluoroacetate derivatives using the procedure described by Silfer et al. (1991) and Macko et al. (1997). Briefly, 0.5 mL of acidified 2-propanol was added to the vials. They were then re-sealed with their teflon-lined caps and heated (100^{o}C) for 1 hour to esterify the amino acids. Subsequently, the samples were immediately placed in a freezer to quench the reaction. Once cooled, the isopropanol was evaporated under a

stream of pre-purified N_2. To remove excess isopropanol and water, CH_2Cl_2 (0.25 mL) was added twice and evaporated with N_2 after each addition. CH_2Cl_2 and trifluoroacetic anhydride (TFAA) were then added (0.5 mL each), the vials sealed and heated (100^oC) for 10 minutes to acylate the amino acid isopropyl esters. After cooling, the vials were placed in an ice bath where the solvent was again evaporated under N_2. Finally, CH_2Cl_2 (0.25 mL) was added and blown off under N_2 to remove any residual TFAA and trifluoroacetic acid. The vials were taken out of the ice bath and remained sealed until analysis was performed, typically within a week.

Gas Chromatography: GC analysis was performed using a Hewlett Packard 5890 gas chromatograph (30 m x .25 mm DB-1 column, 0.25 μm film thickness) equipped with a flame ionization detector (FID). Derivatized THAA samples were dissolved in ethyl acetate; the dilution volumes (~50 μL for *E. huxleyi* cells and ~1 mL for standards) were dependent on the expected amino acid concentrations. An aliquot (1 μL) of this solution was injected into a split/splitless injector (290^oC) operated in splitless mode. The oven was then temperature programmed (75 - 140^oC at 5^o/min, 140 - 270^oC at 10^o/min, 15min hold) to obtain the desired separation of seventeen amino acids and two internal standards. Fig. 2.2A illustrates a representative chromatogram of the standard mixture. The resultant chromatographic data was acquired and quantified using Chrom Perfect (http://www.chromperfect.com) software.

Response Factors: Response factors (RF, amount/area) establish the relationship between the amount of amino acid injected onto the GC and the computer-integrated area for the resultant chromatogram peak. Using standard solutions, response factors (ng/area)

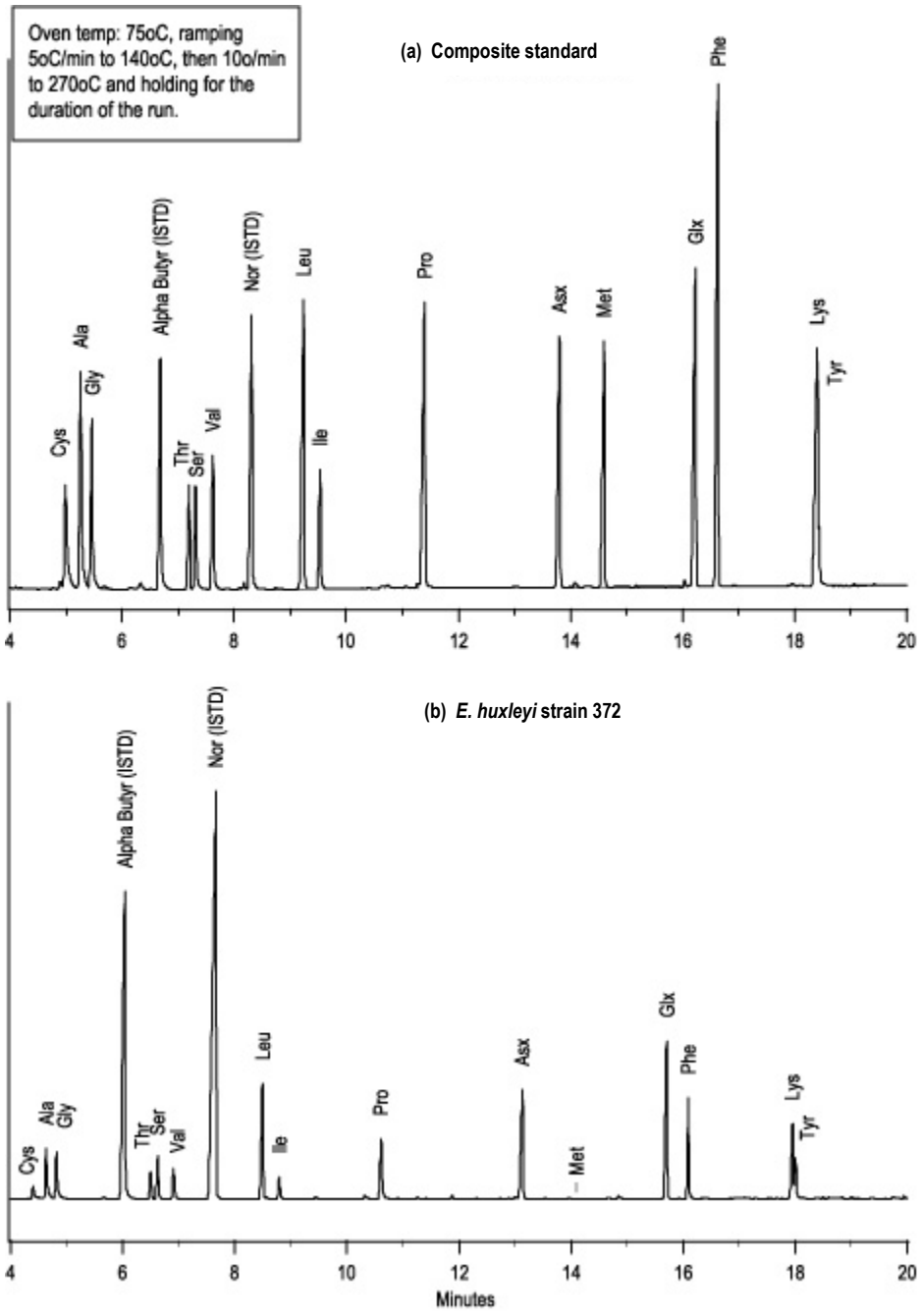

Figure 2.2: Chromatograms generated from GC-FID analysis of a composite amino acid standard (a) and a total amino acid hydrolysate from *E. huxleyi* strain 372 (b). Seventeen amino acids and the two internal standards, α-amino-n-butyric acid (α-Butyr) and norvaline (Nor), were detected using this method. The derivitization process chemically renders glutamine equivalent to glutamic acid (Glx) and asparagine equivalent to aspartic acid (Asx). Arginine, histidine, and tryptophan are not detected using the GC-FID method. The area of each peak was determined by Chrom Perfect software.

were calculated for each of 17 amino acids and the internal standard norvaline. The composite solutions contained 10^{-5} moles or more (total) of amino acid dissolved in 0.1 N HCl. These standards were placed in a reaction vial, blown down under N_2, and then derivatized and analyzed like an experimental sample.

While the RFs of the amino acids were similar, they were not identical. Relative response factors (RRFs) normalize the RF of each amino acid to, in this case, that of the internal standard norvaline (RF_{AA}/ RF_{nor}). Table 2.1 lists the RRFs for the seventeen detectable amino acids, calculated from a composite standard. While most RRFs are close to unity, values range from 0.82 for phenylalanine to 3.43 for cysteine. The cause for the large imprecision for cysteine and tyrosine may be chemical in nature. Cysteine can dimerize to form a disulfide bond, yielding cystine, which as a larger compound would have a longer retention time. However, GC-FID chromatograms of standards containing cysteine show no detectable longer-eluting compound that would correspond to cystine. Tyrosine contains a large benzene ring in its R-group, which may sterically hinder complete derivatization. Both cases may result in low chromatograph areas and thus high RRFs.

Fig. 2.2B illustrates a typical GC-FID chromatogram produced by THAA from experimental samples. Determining the quantity of an amino acid present per cell ($[AA_{cell}]$) is achieved using a commonly employed internal standard method:

$$[AA_{cell}] = [RRF_{AA} \times RF_{istd} \times Area_{AA} \times (dilVol / injVol)] / (volFil * cells/mL) \quad (1)$$

where RRF_{AA} is the relative response factor for a specific amino acid, pre-determined from standard solutions (table 2.1). Chromatographic peaks were integrated to determine

Table 2.1: Relative response factors (RRF, relative to norvaline) determined by gas chromatography with flame ionization detection for a composite standard containing seventeen different amino acids, with RFs defined as mass/area. The RF for norvaline averaged 0.29 ± 0.11 μg/area. The compounds are tabulated in order of their retention time (RT, in minutes). The number of analyses represented by the average is nine.

			RRF	
	Amino Acid	RT (min)	Ave	Stdev
Cysteine	Cys	4.5	3.43	1.2
Alanine	Ala	4.8	1.19	0.05
Glycine	Gly	5.0	1.31	0.07
Threonine	Thr	6.7	1.81	0.15
Serine	Ser	6.8	1.70	0.13
Valine	Val	7.1	1.49	0.05
Norvaline	Nor	7.9	1	---
Leucine	Leu	8.7	0.99	0.02
Isoleucine	Ile	9.0	1.90	0.08
Proline	Pro	10.9	0.92	0.03
Aspartic Acid + Asparagine	Asx	13.4	1.10	0.07
Methionine	Met	14.3	1.49	0.16
Glutamic Acid + Glutamine	Glx	15.9	1.00	0.05
Phenylalanine	Phe	16.3	0.82	0.03
Lysine	Lys	18.1	0.93	0.22
Tyrosine	Tyr	18.2	2.88	1.42
Tryptophan	Trp	---	Not Detected*	
Arginine	Arg	---	Not Detected*	
Histidine	His	---	Not Detected*	

*Indicates amino acids not detected using GC-FID analysis

the area for each amino acid ($Area_{AA}$) and for the internal standard norvaline. Since the amount of norvaline added to the sample is known, its response factor (RF_{istd}, ng/area) can be calculated for each sample injection. Multiplying the first three terms of the equation gives the amount of an amino acid in the injection. To scale the amino acid abundance to the entire sample, this amount is multiplied by the volume of solvent (ethyl acetate) used to dilute the derivatized sample (dilVol, μL), and divided by the injection

volume (injVol; typically 1μL). The amount (ng) of amino acid present in a sample, in this case *E. huxleyi* cells, is given by dividing this result by the volume of sample filtered (volFil, mL) times the cell density (cells/mL).

Since norvaline was added prior to derivitization, any loss of compounds occurring in the subsequent workup procedure will be automatically accounted, assuming that the loss is not compound specific. Preferential loss of low-molecular-weight (LMW) amino acids, e.g. alanine and glycine, would elevate their RRF and yield results that are too high. Table 2.1 demonstrates that RRF values are not systematically higher for the earlier eluting compounds, and do not appear to be measured with greater imprecision. Hence, use of norvaline for recovery-correction appears to be a reasonable approach.

Quantitation: Sample loss that occurs after the addition of norvaline can be quantified. An estimate of percent recovery (% Rec) is made by calculating the amount of norvaline in a sample as perceived by GC-FID analysis and comparing that result to the known amount added:

$$\% \text{ Rec} = (RF_{nor} \times \text{Area}_{smpl} \times \text{dilVol}) / \text{Amt}_{smpl} \times 100 \quad (2)$$

where RF_{nor} is the response factor for norvaline calculated from standards. The percent recoveries for all experimental samples averaged 82 ± 26%. The large range of values is most likely due to differences in handling, for example sample splashing during the evaporation steps in the derivatization process. Loss due to the evaporation process itself, i.e. volatility, has not been found in the laboratory; as previously stated, LMW amino acids (e.g. alanine and glycine) have reasonable RFFs and low standard deviations (see table 2.1).

2.3.2 *The Ninhydrin Method*

This method (Moore, 1968) involves reaction of ninhydrin and its reduced form, hydrindantin, with primary amines located adjacent to a carboxylic acid group (-COOH) to form a dye, called Ruhemann's Purple (figure 2.2). A lithium acetate solution is required to both buffer the reaction and to keep hydrindantin and its reaction product in solution. It should be noted that proline is a secondary amine and is not detected using this method.

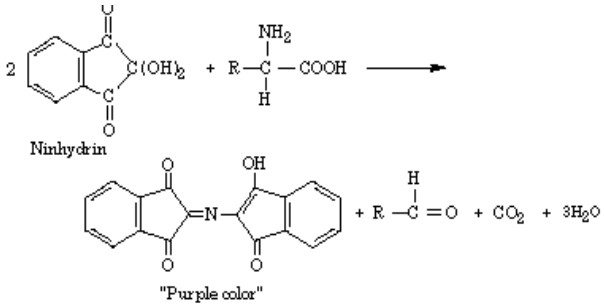

Figure 2.3: Two moles of ninhydrin react with α-amino acids to produce reduced ninhydrin (hydrindantin) and water. The water reacts with the α-amino acid to form an α-keto amino acid and ammonia. This ammonia, ninhydrin, and hydrindantin are what combine to form the purple dye, with an aldehyde and carbon dioxide as by-products. (http://intro.chem.okstate.edu/ChemSource/Forensic/forechem8.htm)

Sample Preparation: Just prior to analysis, the total hydrolyzed amino acid (THAA) sample was transferred from a vial into a 15 mL test tube with either a glass stopper or a Teflon-lined cap. The vial was rinsed with 0.1 N HCl (3x, 1 mL total) to assume quantitative transfer of the sample. Strict adherence to this protocol ensured that changes in concentration among ninhydrin samples were due to sample differences, and not a dilution effect. In the case of standards, individual amino acids were dissolved in 0.1 N HCl to generate final concentrations of 0.1 to 1 mM. Likewise, each standard

solution (1 mL) was then transferred to a capped test tube prior to analysis. A blank containing only 0.1 N HCl was also prepared.

Procedure: The ninhydrin procedure was adapted from Moore (1968), and required both a lithium acetate buffer and a ninhydrin/hydrindantin reagent. Briefly, the lithium acetate buffer was made by the addition of 16.8 g of LiOH to 40 mL of deionized water (DIW). This solution was stirred and acetic acid (29.3 mL) was added after roughly half the LiOH had been dissolved. The final solution volume was adjusted to 95 mL by an appropriate addition of DIW. Two mL of this solution was then diluted 1:3 by addition of DIW (4 mL). LiOH (1g) or acetic acid (1 mL) was added to the buffer solution as needed to adjust the pH of the diluted solution to 5.2.

The ninhydrin/hydrindantin reagent was prepared by the addition of 1 g ninhydrin to dimethylsulfoxide (DMSO) that had been bubbled with N_2 to eliminate oxygen and reduce deterioration of the reagent. Once dissolved, hydrindantin (0.2 g) was likewise added and dissolved with a magnetic stirrer. To the solution, 12.5 mL of the lithium acetate buffer was added, turning the ninhydrin reagent a deep red color. The reagent is stable for about 2 weeks in the dark and was stored under N_2 when not in use.

Spectrophotometry: Prior to analysis, 0.5 mL of the ninhydrin/hydrindantin reagent was added to the 1 mL of THAA sample and vortexed to mix. The sample was then heated (100^{o}C, 15 min), placed in the dark, and allowed to cool at room temperature (15 min). After adding 1:1 ethanol:DIW (10 mL), the sample tube was shaken (1 min). Color in the samples was then ready to be read on the UV/VIS spectrophotometer (Milton Roy Spectronic 301), set at a wavelength of 570 nm and zeroed with a 1:1 ethanol:DIW solution. Calibration curves for each amino acid were constructed using four standard

Table 2.2: Response factors for amino acids analyzed by the ninhydrin method. The correlation coefficient (r^2) for each calibration is also given. Standards for cysteine, isoleucine, proline, phenylalanine, and tryptophan were unavailable at the time of these tests.

AA Std	RF	r^2
Cys	N/A	
Ala	1.86	1.000
Gly	1.77	0.999
Thr	1.79	0.998
Ser	1.91	1.000
Val	1.94	0.999
Leu	1.86	1.000
Iso	N/A	
Asp	1.67	1.000
Met	1.84	1.000
Pro	N/A	
Glu	1.90	1.000
Phe	N/A	
Lys	1.71	1.000
Tyr	1.94	0.999
Trp	N/A	
Arg	1.79	1.000
His	1.78	0.999
average:	1.83	
StDev:	0.082	
Error:	4.5%	

concentrations and a blank. Response factors (absorbance/mM) are defined by the slope of each linear calibration curve (table 2.2). As ninhydrin reacts only with primary amines adjacent to a carboxylate groups, effectively all protein amino acids (with the exception of proline) gave the same response factor (1.83 ± 0.08 absorbance/mM) regardless how many nitrogen atoms the compound contains.

2.4 POC and PN Determination

Prior to analysis of particulate organic carbon (POC) and nitrogen (PN) in each experimental sample, the filters containing the *E. huxleyi* cells, along with a filter blank,

were fumed in a dessicator with concentrated HCl (24 hours) to remove any traces of inorganic carbon in the form of calcium carbonate (Hedges and Stern, 1984). The filters were then folded into pellets and encased first in silver foil and then in tin foil. Eight to ten cysteine standards (29.99% C, 11.66% N), ranging from ~0.05 mg to 0.5 mg, were measured into tin foil boats and also encapsulated. The samples and standards were then run on a Carlo Erba NA-1500 CNS elemental analyzer equipped with a thermal conductivity detector and set up as described by Verardo et al. (1990). The resultant data was recorded on a computer using Chrom Perfect software. Calibration curves for nitrogen and carbon were generated using the cysteine standards. Experimental samples were corrected for the filter blank, which gave values of ~6.4 μg/filter for carbon and ~1.4 μg/filter for nitrogen. This level of blank corresponded to a correction ranging from 4.5 to 21.6% for carbon and nitrogen, depending upon when the samples were collected in the growth curve and during the dark period. Elemental analyses were typically done with a precision of ±1.5% for carbon and ±3% for nitrogen.

2.5 Alkenone Determination

The alkenone content of experimental *E. huxleyi* cells was determined using the procedure described in Prahl et al. (1988) with some minor procedural modifications. Filters for alkenone determination were placed in specialized stainless steel cells that had been filled with CH_2Cl_2/methanol-cleaned Ottowa sand. A standard solution containing nonadecan-10-one and ethyl tricontianoate (10-20 ng/μL) was added (50 μL) as internal recovery standards. The cells were capped and then placed in a Dionex Automated Solvent Extractor (ASE 200, Sunnyvale, CA). The system was heated to 100^{o}C at 1500

psi and samples subsequently extracted (4x, 5 min each) with a 3:1 CH_2Cl_2:methanol mixture (30 mL total). The extracts were collected, combined, and, after addition of water (10 mL), partitioned into hexane (3x, 20 mL total) using a separatory funnel. The combined hexane layers were dried first by washing against 50% NaCl saturated water and then by storage over anhydrous Na_2SO_4 for at least an hour to sometimes as much as overnight.

Dry hexane extracts were concentrated either by standard rotary evaporation or by use of a TurboVap II evaporator (Zymark, Hopkinton, MA). The resultant total extractable lipid (TEL) residues were then transferred quantitatively using CH_2Cl_2 to a one dram vial and the solvent subsequently evaporated to dryness under a stream of purified N_2. A solution containing three external standards (hexamethylbenzene, 3-methyl heneicosane, and n-hexatriacontane) was then added to dissolve the sample, evaluate the GC performance and facilitate quantitation. An aliquot (1 μL) of the solution was injected onto an HP6890A GC equipped with an HP-5 capillary column (60 m x 0.32 mm i.d., 0.25 μm film thickness), a cool on-column injector, and a flame ionization detector. Data acquisition was made possible using Chrom Perfect software. All quantitative alkenone results were corrected for analytical recovery using nonadecan-10-one as the internal recovery standard. Percentage recoveries averaged 82 ± 11% for the first set of experiments in February 2004, and ~70 ± 17% for the second set of experiments in May 2004. A fatal contamination problem caused by accidental exposure of samples to parafilm prevented alkenone analysis in the third set of experiments in September 2004.

Results

3.1 GC-FID Optimization

A reliable method for not only analysis of total hydrolysable amino acids (THAA) but also amino acid composition is essential in order to answer the three key questions posed in the introduction. For this reason, I invested effort to bring a published GC-FID method reliably on-line in our laboratory. Doing so required accomplishing three objectives: learning and adapting the chemical procedure, determining that the method was reproducible, and most importantly, assessing the accuracy of the GC-FID method.

In order to achieve these goals, bovine serum albumin (BSA) was chosen as a key analytical standard. BSA is a well-documented protein that has been fully sequenced (Hirayama et al., 1990). Its analysis via the GC-FID method allowed (1) two different hydrolysis procedures to be tested in order to determine which gives the higher yield, (2) assessment of quantitative reproducibility through measurement of replicate BSA samples, and (3) an estimate of accuracy to be made since accepted literature values exist for the individual amino acid composition of BSA. In addition, BSA was used to evaluate how well the combined quantitative amino acid results from the GC-FID method matched those for THAA (less proline) obtained using the independent ninhydrin method.

Table 3.1 presents the results of BSA analysis by the GC-FID method. Amino acid concentrations were calculated using a variation of equation (1) (see section 2.3.1), where (mgBSA) is the amount of BSA used in the analysis, and [AA] is the amount of amino acid per mg BSA:

$$[AA] = [RRF_{AA} \times RF_{nor} \times Area_{AA} \times (dilVol / injVol)] / (mgBSA) \qquad (1)$$

Table 3.1: Amounts of individual amino acids present in BSA (nmol/mg BSA). Literature values (Hirayama et al., 1990) were compared to values generated from GC analysis of BSA using two different hydrolysis methods (Hydrol 1 and Hydrol 2, in triplicate). RelErr is the standard deviation divided by the average, % of Lit is the average assessed in the present work divided by the literature value. Total amino acid (or THAA) abundances and literature totals for the GC-FID method (bold) and the ninhydrin method do not include undetectable amino acids. RelErr for the GC-FID total was calculated using propagation of error.

	BSA	Hydrol 1 (150oC/1hr)			Hydrol 2 (100oC/24hrs)		
Amino Acid	Literature	Ave	RelErr	% of Lit	Ave	RelErr	% of Lit
Cys	528	195	19%	37%	291	1%	55%
Ala	724	635	21%	88%	504	23%	70%
Gly	256	174	4%	67%	163	21%	63%
Thr	513	549	22%	107%	401	8%	78%
Ser	482	459	9%	95%	346	30%	72%
Val	573	257	21%	45%	171	13%	30%
Leu	980	1034	2%	106%	968	10%	99%
Ile	226	83	34%	37%	57	14%	25%
Pro†	422†	460	4%	109%	460	11%	109%
Asx (Asp + Asn)	829	791	6%	96%	782	10%	94%
Met	75	---			---		
Glx (Glu + Gln)	1191	1480	6%	124%	1446	10%	122%
Phe	452	530	6%	117%	507	11%	112%
Lys	904	1220	11%	134%	1120	10%	123%
Tyr	317	128	24%	40%	57	84%	18%
Arg*	392*	Not Detected			Not Detected		
His*	241*	Not Detected			Not Detected		
Trp*	45*	Not Detected			Not Detected		
GC-FID Total	**8472**	**7995**	**3%**	**94%**	**7275**	**4%**	**86%**
Ninhydrin	8728	6744	22%	77%	6758	30%	77%

--- Below GC-FID detection limits.
† Not included in literature total for the ninhydrin comparison.
* Not included in literature total for the GC-FID comparison.

BSA samples were analyzed in triplicate using hydrolysis method 1 (150^{o}C for 1 hour: Cowie and Hedges, 1992) and method 2 (100^{o}C for 24 hours: Engel and Hare, 1985). In each case, the results were averaged and the relative standard deviation (RelErr, standard

deviation divided by the average) was calculated for each amino acid. Note that nine of the fourteen amino acids values quantifiable for the GC-FID method had lower values of RelErr using hydrolysis method 1.

In table 3.1, literature values for amino acid abundances in BSA are listed (Hirayama et al., 1990). In order to best evaluate results from the two hydrolysis methods, amino acid abundances determined by the GC-FID method for each hydrolysis approach were divided by the literature values (% of Lit). Results from hydrolysis method 1 better approximated the literature amounts for eight of the fourteen listed amino acid values. Consequently, hydrolysis 1 was selected as the method of choice for analysis of all the experimental samples.

The accuracy of the hydrolysis 1 method was assessed using a 2-sample t-test (Berry and Lindgren, 1996) to compare the GC-FID results to the literature. Calculations determined a statistical match for alanine, threonine, leucine, and proline ($p<0.05$). Despite the lack of statistical similarity for the other amino acids, the determined amino acid abundances were summed to yield a measure of THAA. GC-FID analysis using the hydrolysis 1 method generated a THAA value of 7995 nmol/mg BSA, which described 94% of the literature total for the GC-FID detectable amino acids, a reasonable match. Relative error for the THAA value was defined as

$$\mathrm{RelErr}_{(\mathrm{THAA})} = [\Sigma(\sigma^2)]^{1/2}$$

where σ is the standard deviation (Ave*RelErr) for each amino acid (Lindberg, 2000). The relative error for the GC-FID method was 3% for hydrolysis 1, relatively small. Using the literature values as a benchmark, the data show that the GC-FID method is a sufficiently accurate and reproducible means of quantifying THAA.

The ninhydrin method gave a second, independent THAA measure which provides a quantitative check on the assessment by the GC-FID method. Results from analysis of THAA generated from BSA by the hydrolysis one method describes 77 ± 22% (three replicates) of the literature value, which includes all amino acids except proline (Ninhydrin, table 3.1). The yield for the ninhydrin analysis is notably lower, and the relative error higher, than that for the GC. However, while the GC-FID method corrects for loss during the derivitization procedure by the use of the yield-tracer norvaline (section 2.3.1), ninhydrin samples are not recovery-corrected. The correction for the GC-FID method averaged 18% for hydrolysis 1, roughly the difference between the THAA totals for the GC-FID and ninhydrin methods. Ninhydrin analyses of experimental replicates have only 0.4% (four replicates) and 1.1% (excluding one outlier, three replicates) relative error. Ninhydrin values match GC values to an average of 89 ± 24% for all experimental samples, which indicates that the two methods agree quite well with each other, thereby providing a viable means of determining THAA amounts.

3.2 Nitrogen Dynamics during Continuous Darkness

Dark experiments were conducted with *E. huxleyi* strains 1742 and 372. During the experiments, the movement of nitrogen was tracked by monitoring media nutrients, total particulate nitrogen (PN), and amino acids (THAA). These measures were used to validate the findings of previous dark experiments (Fig. 1.1 and 1.2) and to address the nitrogen-related portion of the first question posed in the introduction: are *E. huxleyi* cells manufacturing amino acids in prolonged darkness using media nitrate and cellular alkenone carbon?

Results are summarized in table 3.2, along with phosphate concentrations and cell counts. No experiment was conducted with strain 372 in the first experiment (February 2004). Cell counts (cells/mL) show that once cells were shifted to darkness (shaded regions), growth stopped after one day in all cases, as previously observed (Figs. 1.2 and 1.3). During this dark period, strain 372 showed no drawdown of nitrate (NO_3^-) or phosphate (PO_4^{-3}) and no increase in PN, in agreement with previous experiments with both CCMP 372 (Fig 1.2) and CCMP 370 (Appendix A). Based on the previous lack of nitrate drawdown, no amino acid accumulation was expected in strain 372, and none was found. Results from amino acid analysis via the GC-FID (GC AA) and ninhydrin (Nin AA) methods both showed no change in THAA levels during the dark period.

Strain 1742 did display nutrient drawdown, specifically nitrate, during continuous darkness in previous experiments (Fig 1.1), suggesting that strain 1742 may be capable of dark-period THAA accumulation. Dark-period levels of combined nitrate plus nitrite (N+N) in my experiments with strain 1742 were fitted with a linear regression and an F-statistic, t-value and subsequently a p-value were calculated in order to test the hypothesis that the slope of the trendline was zero (Berry and Lindgren, 1996; R v. 2.4.0). This analysis revealed that the first experiment (February) was the only one that displayed a definitive nitrate drawdown ($p = 0.004$, H_o: slope = 0). Nitrate concentration in the media decreased steadily by 18% over the course of five days. The second experiment (May) with strain 1742 demonstrated a minor decrease (5%) which was somewhat significant ($p = 0.011$), while the third experiment (September) showed no decrease ($p = 0.49$).

Table 3.2: Particulate nitrogen (PN) and total amino acid (THAA) concentrations determined via both the GC-FID (GC AA) and ninhydrin (Nin AA) methods (both fmol/cell) for strains 1742 and 372. The strains were grown in media (□M) containing nitrate (NO_3^-), nitrite (NO_2^{-2}), and phosphate (PO_4^{-3}). Shaded regions depict periods of continuous darkness. GCN quantifies the total nitrogen represented by the sum of individual amino acids detected by GC-FID analysis. Individual amino acid abundances are listed in appendix B.

Strain 372

		(fmol/cell)				MEDIA (μM)		
Day	cells/mL (E+5)	GC AA	Nin AA	GC N	PN	NO_3^-	NO_2^{-2}	PO_4^{-3}
#2 (May)								
1	2.0					79	0.2	3.7
2	2.5	46	N/A	82		72	0.3	3.0
3	2.5	35	N/A	55	---	69	0.4	2.9
4	2.6	41	N/A	62	---	69	0.3	2.8
5	2.2	32	N/A	49	---	69	0.3	2.6
6	2.5	39	N/A	60	---	69	0.3	2.6
7	2.5	35	N/A	57	---	68	0.3	2.5
#3 (Sept)								
2	3.9	22	13	37	59	65	0.3	0.6
3	5.7	26	25	39	44	62	0.3	0.3
4	5.4	26	23	36	50	62	0.3	0.1
5	5.7	23	22	33	*	62	0.3	0.2
6	5.5	*	23	*	*	59	0.3	0.2
7	5.7	22	22	35	42	62	0.3	0.1

--- Blanking error, values rejected.

*Suspicious value, cause unknown. Rejected.

Table 3.2 (continued)

Strain 1742

Day	cells/mL (E+5)	(fmol/cell) GC AA	Nin AA	GC N	PN	MEDIA (µM) NO_3^-	NO_2^{-2}	PO_4^{-3}
#1 (Feb)								
1	1.6				46	80	N/A	3.5
2	2.5	23	38	36	45	74	N/A	3.0
3	3.2	25	43	39	50	70	N/A	2.6
4†	3.1	30	46	49	59	66	N/A	2.4
5	3.4	34	47	56	60	63	N/A	2.2
6	3.5	39	52	65	73	58	N/A	2.1
7	3.5	**	54	**	80	57	N/A	1.9
#2 (May)								
1	1.5				114	85	0.1	N/A
2	2.6	20	24	31	68	80	0.2	3.2
3	2.4	26	26	41	74	77	0.3	3.0
4	2.3	27	29	44	79	77	0.2	3.0
5	2.3	27	28	47	88	76	0.2	2.9
6	2.6	27	29	44	---	74	0.1	2.9
7	2.5	28	29	45	---	73	0.1	2.7
#3 (Sept)								
1	1.8	26	54	41	58	80	0.3	1.5
2	3.5	22	28	36	51	71	0.6	0.9
3	4.0	18	24	29	49	71	0.4	0.7
4	3.9	21	27	34	52	67	0.3	0.8
5	4.2	21	26	34	53	70	0.3	0.8
6	3.9	24	30	37	52	72	0.3	0.8
7	4.3	24	27	38	52	71	0.3	0.8

--- Blanking error, values rejected.

**Low hydrolysis volume. Sample rejected.

†GC and Nin samples went unfrozen for 24 hrs after collection.

If nitrate in the media is being used to synthesize amino acids during continuous darkness, the drawdown of N+N in the February experiment with strain 1742 should correspond to an increase in cellular THAA. Indeed, statistical analysis showed that the first experiment displayed a significant increase in THAA during continuous darkness ($p < 0.001$ and < 0.003 for the GC-FID and ninhydrin methods, respectively; H_o: slope = 0), while the second and third experiments displayed at most only a minor increase ($p = 0.04$ and 0.02 for both methods, respectively). The first experiment was the only one to display a significant dark-period increase ($p = 0.001$) in PN, a finding that parallels the observation for THAA. The partial data for the second experiment was inconclusive, while results for the third experiment displayed a minor increase ($p = 0.02$), again consistent with the THAA findings.

The results show that in the experiment when combined nitrate and nitrite (N+N) drawdown occurred, amino acid (THAA) levels increased. And, when no significant nitrate drawdown occurred, THAA levels remained constant. This pattern suggests that nitrate uptake in continuous darkness is tied to THAA synthesis. While these findings speak to the first question, the second question posed in the introduction can also be addressed: is CCMP 1742 a physiologically unique strain of *E. huxleyi* with respect to cellular nitrogen dynamics? Nutrient drawdown and PN increases during continuous darkness have been shown to occur in strain 1742, and the experiments here suggest that this phenomenon is linked with THAA accumulation. On the other hand, strain 372 has exhibited no such dark-period behavior. This finding suggests that CCMP1742 is behaving different physiologically different and potentially may be a unique strain. But,

the differences among the three experiments with CCMP1742 conducted in this work suggest that its behavior is dependant on some as yet unclearly specified external factor.

When the data allowed, PN and residual N+N were summed to give a total amount of nitrogen (ΣN) in the experimental flasks (table 3.3). Given a closed system, any nitrogen in the form of N+N that disappears from the media should end up in either the cells (PN) or in another dissolved form (e.g. ammonia or dissolved organic nitrogen). Throughout each experiment, the sum of N+N and PN remains constant, suggesting that these are the dominant forms of nitrogen in the system. Species such as ammonia or dissolved organic nitrogen are minor at most.

Table 3.3: PN, N+N, and their sum (ΣN) for all experiments (μM). Shaded regions are during continuous darkness. Note that PN here is a molar quantity.

Strain 372

#2 (May)				#3 (Sept)			
Day	PN	N+N	ΣN	Day	PN	N+N	ΣN
1	*	79	*	1			
2	*	72	*	2	23	65	88
3	*	69	*	3	25	62	87
4	*	69	*	4	27	62	89
5	*	69	*	5	**	62	**
6	*	69	*	6	**	59	**
7	*	68	*	7	24	63	87

Strain 1742

#1 (Feb)				#2 (May)				#3 (Sept)			
Day	PN	N+N	ΣN	Day	PN	N+N	ΣN	Day	PN	N+N	ΣN
1	7	80	87	1	17	85	102	1	10	80	90
2	11	74	85	2	18	80	97	2	18	72	89
3	16	70	86	3	18	77	95	3	20	71	91
4	18	66	84	4	18	77	95	4	20	67	87
5	20	63	84	5	21	76	97	5	23	70	92
6	26	58	84	6	*	74	*	6	20	72	92
7	28	57	85	7	*	73	*	7	22	71	93

*Data excluded due to problem with filter blank; possible nitrogen contamination caused elevated values.
**Values suspect due to elevated nitrogen levels. Rejected and not included in discussion.

3.3 Amino Acid Composition

With the exceptions of arginine, histidine, and tryptophan, the use of the GC-FID method provides a way to define the amino acid composition of *E. huxleyi* and answer the third question posed in the introduction: if amino acids are biosynthesized in prolonged darkness by certain strains of *E. huxleyi*, is the biosynthesis compound-specific?

Table 3.4 summarizes the individual amino acid composition measured for each experiment, subdividing results into those for light-receiving cells and cells shifted to darkness. For these two treatments, an average abundance was calculated for each amino acid. For every individual amino acid, a two-sample t-test was used to test whether the average for the light-receiving cells was equal to the average of the dark-shifted cells (Berry and Lindgren, 1996). The resultant p-values revealed that in the case of all experiments, a shift to darkness had no effect on the individual amino acid composition (all $p > 0.18$; H_o: $\mu_1=\mu_2$). In addition, an average amino acid composition was computed for all dark-shifted samples in all experiments for both strains 1742 and 372. A two-sample t-test showed that the dark-period amino acid composition did not differ among experiments (all $p > 0.17$; H_o: $\mu_1=\mu_2$).

Fig 3.1 shows a comparison of the individual amino acid composition observed for all light-receiving samples for strain 1742 with that for samples taken during darkness. The molecular composition between the two groups is effectively indistinguishable. This observation indicates that for the compounds detectable by the GC-FID method, at least, that the amino acid accumulation apparent for strain 1742 in the

Table 3.4: The average amino acid composition in terms of mole fractions, divided between light-receiving (Light) and dark-shifted cells (Dark, shaded regions) for each experiment (Exp) with both strains. 'n' refers to sample size.

Strain	Exp	n	Light/Dark		Cys	Ala	Gly	Thr	Ser	Val	Leu	Iso	Pro	Asp	Met	Glu	Phe	Lys	Tyr
1742	#1 (Feb)	3	Light	Ave		14%	9%	4%	6%	4%	9%	2%	7%	12%	3%	19%	6%	7%	1%
				Stdev		5.9%	0.5%	1.3%	1.8%	0.6%	0.8%	1.5%	0.9%	2.2%	—	3.9%	0.7%	0.7%	0.5%
		5	Dark	Ave		13%	10%	4%	6%	3%	9%	2%	7%	11%	2%	18%	6%	7%	2%
				Stdev		1.9%	0.6%	1.3%	1.3%	0.4%	0.5%	0.3%	0.4%	1.7%	0.5%	3.1%	0.3%	0.5%	0.7%
	#2 (May)	2	Light	Ave	3%	8%	9%	5%	6%	5%	9%	4%	6%	12%	2%	15%	5%	8%	3%
				Stdev	0.3%	4.6%	2.0%	0.3%	1.8%	1.6%	0.4%	0.2%	0.2%	1.5%	—	1.6%	0.5%	0.9%	3.6%
		5	Dark	Ave	2%	10%	12%	4%	5%	6%	11%	5%	7%	13%		15%	6%	7%	1%
				Stdev	0.6%	2.7%	0.9%	1.5%	—	1.3%	0.5%	0.7%	1.0%	1.7%		1.6%	0.7%	1.3%	0.7%
	#3 (Sept)	4	Light	Ave	2%	11%	11%	4%	5%	6%	11%	4%	7%	12%		15%	5%	5%	2%
				Stdev	1.2%	1.4%	1.3%	1.6%	1.9%	0.4%	0.8%	0.5%	0.6%	0.7%		0.8%	0.6%	1.8%	0.5%
		5	Dark	Ave	2%	12%	12%	3%	5%	6%	11%	4%	7%	13%		15%	5%	5%	2%
				Stdev	0.6%	1.0%	0.6%	1.3%	1.6%	0.7%	0.2%	0.4%	0.3%	0.3%		0.5%	0.2%	0.9%	0.5%
372	#2 (May)	2	Light	Ave	4%	11%	11%	4%	5%	7%	11%	5%	6%	12%	1%	14%	5%	5%	2%
				Stdev	2.7%	0.6%	1.7%	2.3%	3.0%	1.6%	0.7%	1.2%	1.0%	1.7%	0.3%	1.4%	0.7%	0.3%	1.3%
		5	Dark	Ave	3%	10%	10%	4%	7%	6%	11%	5%	7%	13%	1%	14%	6%	5%	3%
				Stdev	1.0%	2.4%	0.9%	1.1%	0.6%	1.4%	0.9%	1.0%	0.7%	1.8%	—	3.0%	1.2%	1.1%	1.8%
	#3 (Sept)	2	Light	Ave	2%	8%	10%	3%	5%	5%	11%	3%	7%	13%		16%	5%	6%	2%
				Stdev	1.3%	4.3%	2.8%	0.4%	4.6%	1.5%	0.4%	0.7%	0.4%	1.4%		3.1%	0.9%	0.3%	3.0%
		5	Dark	Ave	2%	9%	9%	5%	7%	5%	10%	4%	7%	11%	4%	13%	5%	5%	4%
				Stdev	0.9%	1.3%	0.4%	0.7%	1.1%	0.5%	0.3%	0.4%	0.5%	1.2%	0.0%	0.4%	0.1%	0.6%	1.2%

— One data point, standard deviation could not be computed.

Open boxes were below minimum detection level; no data available

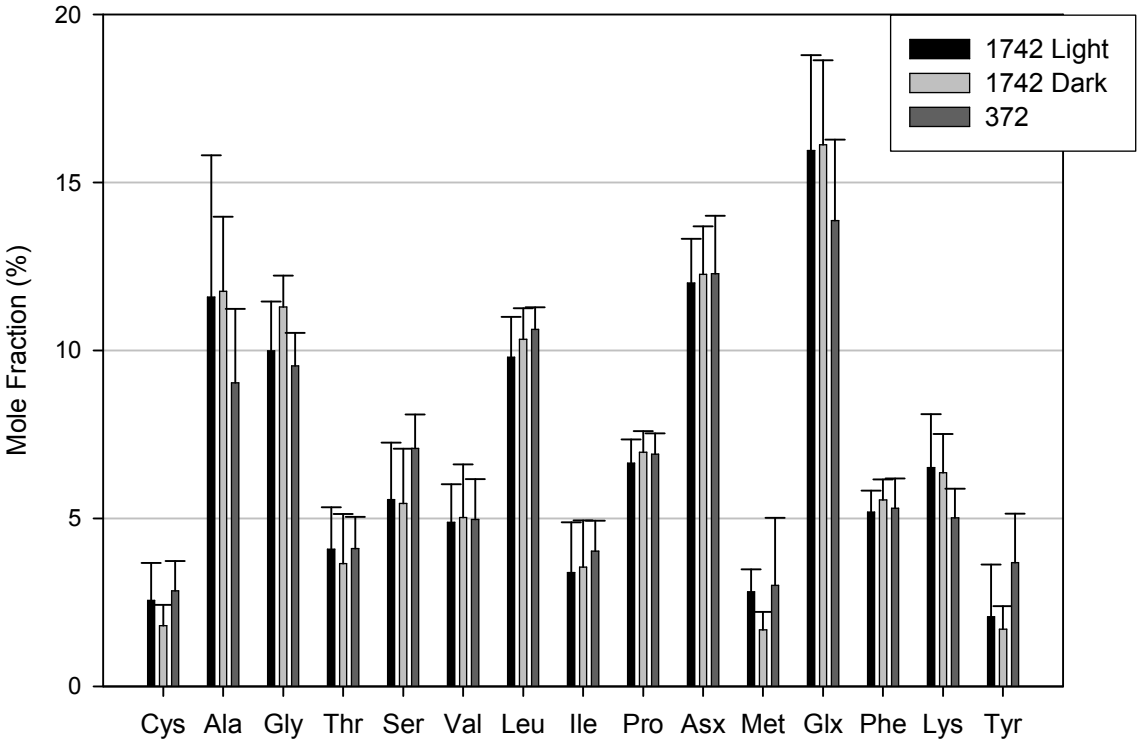

Figure 3.1: The averaged amino acid composition for *E. huxleyi* strains 1742 and 372. The average composition for strain 1742 has been calculated for both cells receiving light and those experiencing continuous darkness, with (n = 9 and 15, respectively). Strain 372 is shown as an average of both (n=14). Statistical analysis showed no compositional differences between light and dark treatments for any of the amino acids, for either strain 1742 or 372 (partitioning into light and dark treatments not shown). There was also no compositional difference between the two strains when an average for all samples was compared (n = 24 and 14 for strains 1742 and 372, respectively).

first experiment is not compound-specific. Moreover, a comparison of the average amino acid compositions of strains 1742 and strain 372 (Fig. 3.1) demonstrates that the two strains behave similarly (all $p >> 0.17$).

3.4 THAA Nitrogen

To further evaluate the THAA data and the nitrogen dynamics in *E. huxleyi*, calculations were made to determine how much of the cellular nitrogen pool (PN) is accounted by amino acids. Using the results from the GC-FID method, the amount of nitrogen in each amino acid was calculated, summed, and the total listed as GC-N in table 3.2. This value was then divided by PN to generate the percent of amino acid nitrogen comprising total particulate nitrogen.

Focusing on the period of continuous darkness, results from this calculation for each experiment with *E. huxleyi* are shown in Fig 3.2. As a benchmark, a total hydrolysable amino acid (THAA) to total nitrogen ratio value of 70% was used, representing the average of values measured in six phytoplankton (*Dunaliella euchlora*, *Nitzschia closterium*, *Skeletonema costatum*, *Amphidinium carterae*, *Thalassiosira weissflogii I* and *II*; Cowie and Hedges, 1992). The benchmark is represented in Fig 3.2 as a dashed line, with the shaded area around it corresponding to the range of the published values (68 to 79%).

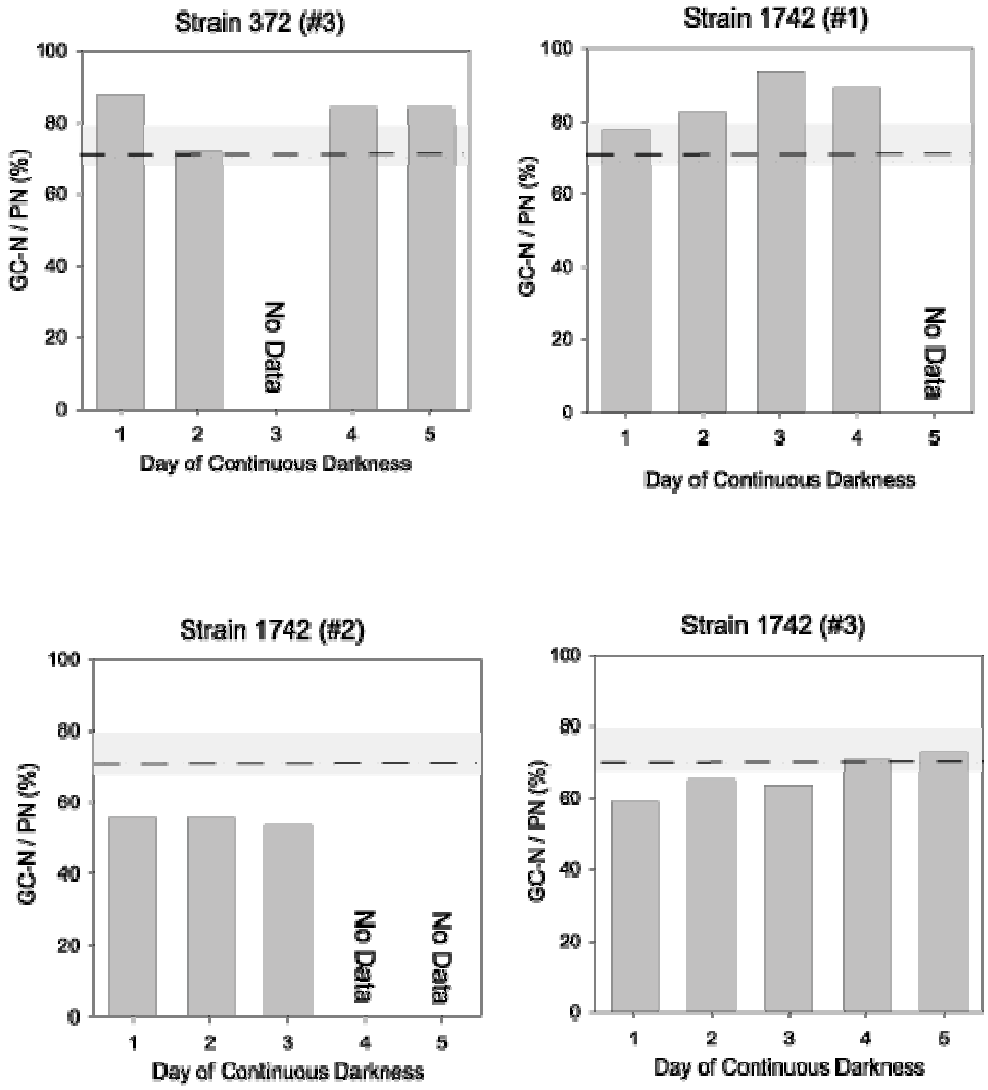

Figure 3.2: Percent of THAA nitrogen as determined by the GC-FID method (GC-N) that comprises total nitrogen (PN) for all experiments with both strains 1742 and 372, when data was available. The dashed line represents a benchmark value of 70% (Cowie and Hedges, 1992), an average for six phytoplankton ranging from 68 to 79% THAA-N/PN (shaded area). The GC-N/PN values for strain 372 and the first experiment with strain 1742 both exceed the published value. Values for the third experiment with strain 1742 near 70%, while those for the second experiment fall short by ~15%. As ninhydrin values match GC-FID values to an average of 4% in the second experiment, suggesting the underestimation is not due to an error in the amino acid data.

In strain 372 (#3; September), the proportion of THAA-N to PN remained relatively constant during the continuous darkness period and above the benchmark value, averaging 77 ± 11%. In strain 1742, dark-period values of THAA-N/PN for the second experiment (May) were ~15% below the benchmark, averaging 53 ± 5%. However, the proportion of THAA-N to PN for the first (February) and third (September) experiments was near or above the benchmark, averaging 67 ± 5% and 85 ± 7%, respectively. Despite the range of THAA-N/PN values for strain 1742, both strains of *E. huxleyi* were in general agreement with the benchmark range of 68 to 79%. Assuming that "the 'living' portion of all types of cells has about the same gross molecular composition" (Lehninger, 1975) and, consequently, that the ratio of THAA-N to PN is approximately equivalent in all phytoplankton, this suggests that the GC-FID method adequately described the amount of THAA-N in cells.

During the first and third experiments with strain 1742, THAA-N/PN values increased slightly during the dark period. In the third experiment, no significant change in THAA-N or PN content of cells was measured during darkness (section 3.2). The increase in THAA-N/PN was likely an artifact of scatter in the data, especially considering the range of values for strain 372. Conversely, dark-period levels of both PN and THAA-N increased during the first experiment (table 3.2). THAA-N increased by 0.026 pmol/cell by the fourth day of darkness, which is a close match to the PN increase of 0.023 pmol/cell and suggests that the PN increase was due to THAA-N. If so, and if THAA-N was the only fraction of PN that increased, the ratio of THAA-N to PN would have likewise increased as a result.

Analysis of the THAA-N and PN data has therefore indicated that 1) THAA-N described a reasonable amount of PN in the experiments in this work and 2) the dark-period PN increases during the first experiment with strain 1742 were due to amino acid accumulation.

3.5 Alkenone and POC Analysis

The first question posed in the introduction was: are *E. huxleyi* cells manufacturing amino acids during continuous darkness using media nitrate and cellular alkenone carbon? Results have thus far shown that strain 1742 is capable of producing amino acids during continuous darkness, and there is strong evidence that the THAA accumulates at the expense of media nitrate plus nitrite (N+N). To determine whether alkenones play a role in THAA accumulation, both alkenones and total particulate organic carbon (POC) were measured during the experiments with *E. huxleyi* strains 1742 and 372.

Table 3.5 presents the analytical results for POC and alkenones (ΣAlkC), listed in terms of carbon for comparative purposes. In all the experiments with both strains 1742 and 372, cellular alkenone levels decreased during continuous darkness, as observed in previous dark experiments (Figs. 1.1 and 1.2). The alkenone decrease was most prominent in strain 1742 (Fig 3.3a), which had cellular alkenone concentrations at the start of the dark exposure that were roughly double those found in strain 372. In addition, alkenone loss occurred more rapidly in strain 372, which completed its loss by the third day of the dark period. In comparison, strain 1742 displayed a more gradual alkenone loss that extended over the entire dark period. These observations have been made

Table 3.5: Alkenone carbon (ΣAlkC) and POC data (fmol C/cell) for all experiments with strains 1742 and 372, when available. ΣAlkC is the sum of all C_{37}, C_{38}, and C_{39} alkenones (Appendix C, pg/cell), multiplied by the weight percent of carbon in alkenones (0.8) and converted to a molar quantity. There is no alkenone data for the September experiments due to a problem with accidental sample contamination with parafilm. Shaded regions are periods of continuous darkness.

372

	May		**Sept**
Day	ΣAlkC	POC	POC
1	1.9	62	58
2	3.5	60	47
3	2.2	72	37
4	2.1	61	37
5	1.1	69	34
6	0.8	85	35
7	1.0	58	32

1742

	Feb		**May**		**Sept**
Day	ΣAlkC	POC	ΣAlkC	POC	POC
1		99	5.7	65	
2	7.6	68	3.2	41	50
3	6.6	66	4.8	48	33
4	*	*	4.4	52	33
5	4.0	58	3.5	56	36
6	2.4	63	2.6	45	21
7	2.3	67	1.7	46	29

*Sample went unfrozen for 24 hrs after collection, value rejected.

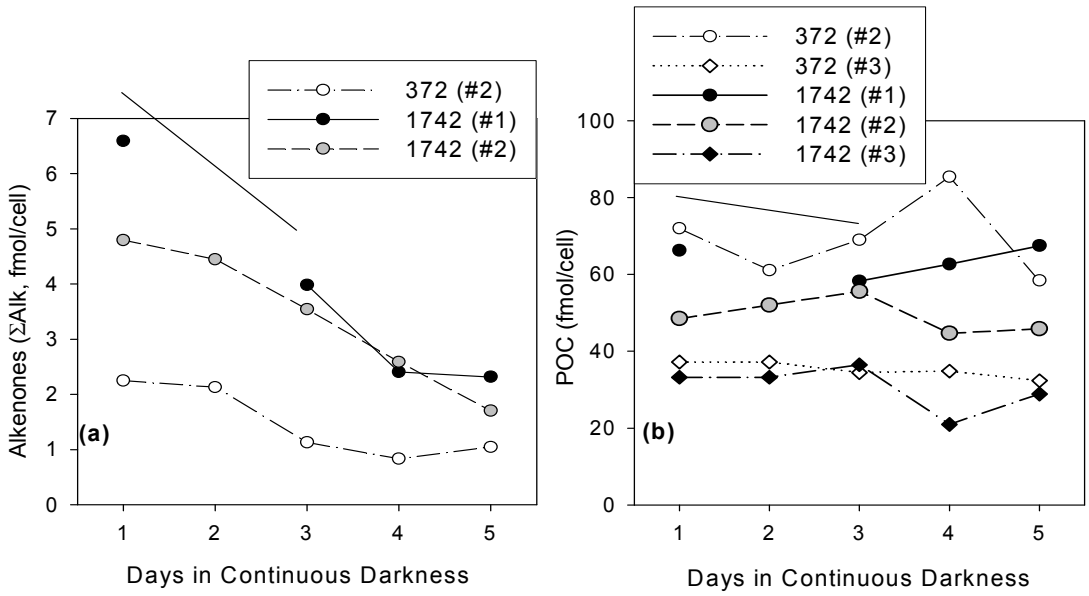

Figure 3.3: Cellular alkenone concentrations during continuous darkness for all experiments with strains 1742 and 372, when data was available. Note that alkenone levels are higher in strain 1742 compared to strain 372, and the dark-period decrease occurs much more gradually in strain 1742, while strain 372 completes its alkenone loss by day three.

previously (Figs. 1.1 and. 1.2, Appendix A) and suggest that strain 1742 may be physiologically unique with regard to its alkenone content and dark-period behavior.

Though alkenone loss occurred in all experiments with both strains, definitive POC decreases were not observed during continuous darkness (Fig 3.3b). Despite the variability in the POC data, no overall loss occurred and no loss of POC during continuous darkness has been observed in previous dark experiments (Figs. 1.1 and 1.2). In the second experiment with strain 372 (May), alkenone carbon decreased alkenone carbon by 0.001 pmol/cell, or ~1.7% of the average dark-period POC (0.069 ± 0.011 pmol/cell), which was not enough to have a noticeable effect on POC levels. The alkenone carbon loss in strain 1742 was more substantial, with a 0.004 pmol/cell decrease during the dark period for the first (February) experiment and an 0.003 pmol/cell decrease for the second (May) experiment. These losses corresponded to 5.9% and 6.3% of the average dark-period POC (0.064 ± 0.004 and 0.049 ± 0.005 pmol/cell), respectively. Despite this magnitude of alkenone carbon loss in these experiments, corresponding POC levels displayed no overall decrease (Fig 3.3b). This observation suggests that during the continuous darkness period in strain 1742, the carbon-rich alkenones were altered into another biochemical form rather than lost as carbon dioxide as a consequence of cell respiration.

Are alkenones being used to form THAA in *E. huxleyi* strain 1742? THAA accumulation occurred only during continuous darkness during the first (February) experiment with strain 1742, and not in any other experiments with this strain. Interestingly, at the start of the dark period, cellular levels of both alkenone carbon and POC were highest in this experiment. If the source of the THAA carbon is alkenones, a

decrease in cellular alkenone levels would be expected only during first experiment. Yet, a decrease in dark-period alkenone concentration seemed apparent in all experiments. In strain 372, the alkenone carbon may have been respired, with the resultant decrease in POC being immeasurable. However, the second (May) experiment with strain 1742 provides evidence that alkenone loss during continuous darkness can occur without an increase in cellular THAA content.

This observation does not preclude alkenones as the source of THAA carbon during the first experiment with strain 1742. However, a simple calculation shows that it is unlikely. During the continuous darkness period in the first experiment with strain 1742, THAA-N and PN increased equally (section 3.4); the increase was ~0.030 pmol N/cell (table 3.3) by the fifth day of darkness. Using the molar C:N ratio for amino acids (3.5; Cowie and Hedges, 1992), the amount of carbon necessary to account for the THAA increase is 0.105 pmol C/cell. The alkenone carbon loss of 0.004 pmol C/cell was not enough to account for the THAA increase. The THAA carbon must therefore come from another, or at least an additional, cellular constituent. Based upon data for other phytoplankton, carbohydrates are the likely candidates (see section 4.1).

Discussion

4.1 Dark-Period Nitrogen Dynamics in Phytoplankton

The design of experiments in this work allowed comparison of the dark-period nitrogen behaviors in two different strains of *E. huxleyi*, CCMP1742 and 372. The results suggest that strain 1742 is physiologically distinct. During continuous darkness, strain 1742 demonstrated nutrient drawdown and an increase in particulate nitrogen (PN) (first experiment, February, table 3.3). Use of the GC-FID and ninhydrin methods has revealed that the dark-period PN increase correlates with amino acid (THAA) accumulation (table 3.2, section 3.4). Though strain 372 did not show any of these characteristics in prolonged darkness, strain 1742 is not the only phytoplankton to experience such dark-period dynamics.

Uptake of nitrate during darkness occurs in diatoms (Cuhel et al., 1984), cyanobacteria (Foy and Smith, 1980), and dinoflagellates (Cullen, 1985). In all three cases, this behavior has been related to buoyancy regulation (van Rign and Shilo, 1985; Villareal and Carpenter, 2002; Cullen, 1985; Richardson et al., 1996, Villareal et al., 1999). A number of phytoplankton have been shown to store carbon-rich carbohydrates during the day, and to catabolized these at night as the nitrate is assimilated, forming protein (Cuhel et al., 1984). The carbohydrates are accumulated during photosynthesis in nutrient-depleted surface waters. The cells then sink into light-depleted but nutrient-rich waters during night, where protein is synthesized at the expense of the carbohydrate, and the cells rise back into light.

Dark-period nitrate uptake is generally accepted to be an adaptation to diel light cycles. However, longer periods of darkness, such as the five days in the experiments here, is not improbable for oceanic algae. In the case of large diatoms, generation times are longer than a day (Richardson et al., 1996; Villareal et al., 1999), and they are able to adapt to vertical migrations lasting many times longer than this (Richardson et al., 1996). A study of *Trichodesmium* at station ALOHA revealed that these cells may potentially have vertical migration cycles with periods of 100-150 days (Karl et al., 1992).

Though coccolith production has been theorized to control buoyancy in *E. huxleyi* (Young, 1994; and references therein) and a motile stage of the organism exists (Green et al., 1996), no evidence of vertical migration has been found. However, dark-period nitrate uptake has been found in non-motile organisms. Paasche et al. (1984) compared two dinoflagellates, neither of which exhibited a propensity for diel migration. They found that *Prorocentrum minimum* was capable of carbohydrate storage and dark-period nitrate uptake whenever nitrate was available, while *Gyrodinium aureolum* could do the latter only after a period of nutrient starvation. It was noted that *P. minimum* was more likely to be found near the thermocline or during upwelling events, while *G. aureolum* was more likely to be found near the surface.

The different nutrient-uptake behavior displayed by the two dinoflagellates in Paasche et al. (1984) may be due to the different light levels they experience. *P. minimum* is found lower in the water column and can take up nitrate during darkness in nutrient-replete conditions while *G. aureolum*, residing at the surface, cannot. This finding may be an indication that high irradiances inhibit dark-period nitrate uptake in nutrient-replete

environments. Irradiance may therefore be a factor in the ability of non-motile organisms, such as *E. huxleyi*, to take up nitrate during darkness.

4.2 Experimental Disparity with Strain 1742

Dark-period nitrate drawdown and an increase in PN were demonstrated both during a previous experiment with strain 1742 at low light (60 μEin/m^2-s, Fig 1.1) and during the first experiment (February) in this work at high light (165 μEin/m^2-s). While this shows that strain 1742 is capable of such dark-period nitrogen dynamics, the second (May) and third (September) experiments at high light did not exhibit either of these behaviors clearly, if at all.

Muggli and Harrison (1996) studied *E. huxleyi* cells that were isolated from the same location as strain 1742 and found that growth rate maximized at a light flux of ~75 μEin/m^2s (16^{o}C; 14:10 light:dark cycle). Moldonado and coworkers (unpublished data) conducted light experiments with strain 1742, and likewise found a maximum growth rate at ~75 μEin/m^2s (Fig. 4.1). A light intensity of 165 μEin/m^2-2, as used in this work, would cause cells to be light-saturated. The fact that nutrient drawdown in CCMP1742 was distinct at 60 μEin/m^2s (Fig 1.1) and absent in two of the three experiments at 165 μEin/m^2s suggests that the increased light intensity may have inhibited dark-period nutrient drawdown in strain 1742. The first experiment (February) with strain 1742 was not inhibited, even though it had been placed at 165 μEin/m^2-s five months beforehand, long enough for the cells to adapt to the higher light level. However, this single disparity does not disprove that a high light intensity inhibited dark-period nitrate uptake.

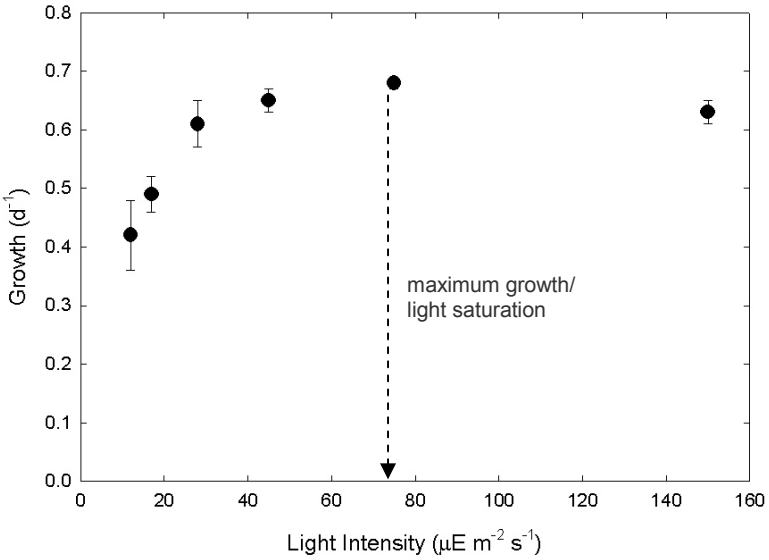

Figure 4.1: A plot of growth (divisions/day) versus light intensity (µEin/m^2s), taken from Moldonado and coworkers (unpublished data) for *E. huxleyi* strain 1742. Growth maximized at a light flux of ~75 µEin/m^2s (dashed arrow). At 60 µEin/m^2s, the light flux used in previous dark experiments, cells are under-saturated, while the light intensity of 165 µEin/m^2s used here is light-saturating for these cells.

Cochlan et al. (1991) conducted shipboard experiments with samples taken in the Strait of Georgia, British Columbia (Canada) to measure nitrate uptake in phytoplankton. They compared surface samples with samples taken from the deep chlorophyll maximum layer (DCML) to study the effect of light, and also compared samples taken from stratified waters to those from a frontal zone to study the effect of nutrient levels. It was found that the ratio of nitrate uptake at night to uptake during the day increased for cells taken from the DCML. In other words, there was an inverse relationship between light levels and dark-period nitrate uptake in the phytoplankton communities. However, Cochlan et al. (1991) noted that this inverse relationship weakened in the presence of nutrient depletion. Surface (high light level) samples taken from stratified waters had a higher rate of dark-period nitrate uptake than those taken from frontal waters. Similarly,

though the higher irradiance in the work here (165 μEin/m^2-s) may have caused a general inhibition of dark-period nutrient drawdown in strain 1742, a period of nutrient-stress could have induced dark-period nitrate uptake during the first experiment.

Maintaining our cell cultures in f/20 media (~100 μM nitrate, ~4 μM phosphate) requires transfers every two weeks (section 3.1), at which time cells are becoming nutrient-stressed and entering stationary phase. While the second (May) and third (September) experiments were inoculated with cells mid-way through the transfer cycle, i.e. a nutrient-replete environment, the first (February) experiment was inoculated from cells transferred two days beforehand. In other words, the cells had probably just experienced nutrient stress. This is also supported by the C/N data (see section 4.4)

Nutrient depletion has been shown to induce dark-period nitrate assimilation in a green flagellate (*Chlamydomonas reinhardtii*), *Thalassiosira weissflogii*, a species of the diatom *Phaeodactylum*, and other algae (Richardson and Cullen 1995; Styrett, 1981 and references therein). Laboratory experiments suggest that by adding a pulse of nitrate, protein synthesis may be initiated at night in some phytoplankton (Cullen and MacIntyre, 1996; and references therein). This effect suggests that by placing nutrient-starved cells of CCMP1742 into a nutrient-replete media, as in the first experiment, dark-period THAA accumulation may have been induced, even though the cells had been growing at a high irradiance level.

E. huxleyi accumulates carbon-rich alkenones when nutrient-stressed (Conte et al., 1998; Epstein et al., 1998; Epstein et al., 2001; Prahl et al., 2003). One day before cells entered continuous darkness, alkenone levels for the first experiment (February) with strain 1742 were roughly twice the levels for the other experiments (table 3.5), suggesting

that nutrient depletion occurred and may still have been having an affect on this experiment. Furthermore, the alkenone data both in this work and previous studies showed that strain 1742 experienced a slow and steady decrease in cellular alkenone levels during continuous darkness. The alkenone loss extended over the entire five-day dark period, whereas the loss in strain 372 was immediate and completed by the third day of darkness (Figs. 1.1, 1.2 and 3.3). As shown in Foy and Smith (1980), cyanophytes that use their carbohydrate reserves more slowly are better able to survive prolonged darkness. If strain 1742 has adapted a slow response to continuous darkness as a survival mechanism, it is also possible that it responds slowly to changes in nutrient levels for the same reason.

The period between the last transfer (nutrient deprivation) and the dark period in the first and following experiments was eleven and sixteen days (roughly seven to nine divisions), respectively. If dark-period nitrate uptake and THAA accumulation was induced in the first experiment and not in the following ones, recovery from nutrient stress would consequently take between eleven and sixteen days in strain 1742. The physiological history of cells may therefore be relevant when investigating dark-period nitrogen dynamics in *E. huxleyi*.

4.3 *Emiliania huxleyi* in the Ocean

I have hypothesized that dark-period nitrate uptake in strain 1742 occurs at low light levels, or at high light levels perhaps after a period of nutrient stress. These same factors have been shown to affect alkenone unsaturation patterns ($U_{37}^{K'}$) (Prahl et al., 2003 and references therein). Clearly, both low light and nutrient deprivation have a

significant impact on the physiology and biochemistry of *E. huxleyi*. The organism may experience both types of stress in its natural environment.

Low nutrient levels are a widespread feature experienced globally by phytoplankton, especially in stratified surface waters. Low light levels can occur as a result of self-shading during algal blooms. In the North Atlantic in 1991, an *E. huxleyi* bloom caused the 1% light level to shoal from >24 m outside the bloom to as low as 8 m within (Holligan et al., 1993). And, living cells can potentially be packaged in aggregates, such as marine snow, and exported from light-replete surface waters to deeper in the euphotic zone (Prahl et al., 2005a).

In addition, there is growing evidence of *E. huxleyi* cells living at low light levels in the deep chlorophyll maximum (DCML), based upon alkenone measurements and the principle that *E. huxleyi* is a dominant alkenone-producer (Prahl et al., 2005b and references therein). Ohkouchi et al. (1999) analyzed alkenones in surface sediments in the central Pacific, and found that in the mid-latitudes (19^{o}-35^{o}N) SST calculated from sediments correlates to water below the surface mixed layer, implying that alkenone export to the sediments originates from the DCML. In the gyre region off the coast of the Oregon/California border in the northeast Pacific, alkenone signatures in the underlying sediments again related to temperatures below the surface mixed layer, indicating alkenone export originates from the DCML (Prahl et al., 1993). As *E. huxleyi* strain 1742 is considered genetically comparable to *E. huxleyi* cells from the central Pacific (Okada and Honjo, 1973), the relationship between light intensity and dark-period nitrate uptake may have implications for cells in systems like these.

4.4 Bacteria and C:N Ratios

Because the cultures used in this study were non-axenic, the possibility of heterotrophic bacterial contamination must be considered, as bacteria may take up nitrate and synthesize amino acids during darkness. Strain 1742 was ordered from the Provasoli-Guillard National Center for Culture of Marine Phytoplankton just five months prior to the first experiment (February). Hence, bacteria could have been present in the original isolate (Shäfer et al., 2002). During the first experiment, the C:N ratios decreased from 13.2 to 8.4 during the dark period (table 4.1). An increase in bacterial biomass, which have a low C:N ratio of ~5 (Nagata, 1986), could have caused or at least contributed to the decrease. However, the bacterial presence would also have to have been present in the second and third experiments with strain 1742, as all the experiments with strain 1742 were inoculated from the same maintained culture. As those experiments did not experience an increase in amino acids or a decrease in C:N ratios, it is unlikely that the C:N decrease in the first experiment was caused by bacteria.

Table 4.1: C:N (atomic) ratios for all experiments, when available. C/N was calculated using PN and POC values. C:N ratios for *E. huxleyi* are ~6.9 to 9, based on previous experiments.

	1742			**372**
Day	**#1**	**#2**	**#3**	**#3**
1	21.5	5.7	10	
2	15.3	6.1	9.3	8.6
3	13.2	6.6	7.6	7.5
4	8.9	6.6	7.1	6.6
5	9.8	6.3	6.4	*
6	8.6	*	6.6	*
7	8.4	*	6.2	6.9

* PN rejected, no C/N value.

E. huxleyi cells have C:N ratios that can range from 5 to 20 (Joassin et al., 2008 and references therein), though previous work with strain 1742 has generated values close to the Redfield ratio of 6.7 (Prahl, unpublished data). Two days before cells entered continuous darkness in the first experiment with strain 1742, C:N ratios were 21.5, very elevated. Such carbon enrichment was not apparent in the second or third experiments with strain 1742, in strain 372, or in the previous experiments at low light (Appendix A). Significantly, the first experiment was the only experiment in this work at high light (165 $\mu Ein/m^2$-s) to take up nitrate and synthesize amino acids during continuous darkness.

As discussed above (section 4.2), pre-dark cellular levels of both POC and alkenone carbon were elevated in the first experiment (February) with strain 1742. This factor may explain the concurrent elevated pre-dark C:N ratios in this same experiment. Both measures suggest that cells in this experiment had experienced nutrient stress as hypothesized (section 4.2) and that dark-period nitrate uptake was therefore induced, despite the high light intensity (165 $\mu Ein/m^2$-s).

4.5 Amino Acid Accumulation

Amino acid (THAA) analysis of the protein standard bovine serum albumin (BSA) showed that the GC-FID (hydrolysis 1) method and the ninhydrin method generated equivalent and reasonable results (section 3.1). Experimental THAA samples analyzed via the ninhydrin matched those analyzed via the GC-FID method to an average of 89 ± 24% (n = 23). During the first (February) experiment with strain 1742, however, the ninhydrin-assessed values are 40% higher than the GC-FID-assessed values during the first dark day (table 3.2), decreasing to 25% higher by the fourth dark day.

The ninhydrin method does not detect proline, which should comprise ~5% of THAA in *E. huxleyi*. This value assumes that the amino acid composition of all phytoplankton are equivalent (Cowie and Hedges, 2002 and references therein), and uses BSA (Hirayama et al., 1990) and *T. weissflogii* (Cowie and Hedges, 1996) as models. Likewise, the GC-FID method does not detect arginine, histidine, or tryptophan, three nitrogen-rich amino acids which should comprise 4%, 3%, and <1% of *E. huxleyi*, respectively. The GC-FID method should therefore only miss ~2% more of the total amino acids (THAA) than the ninhydrin method. This means of assessment suggests that the differences between the two methods in the first experiments with strain 1742 are because arginine, histidine, and/or tryptophan comprised a significant portion of the THAA pool at the onset of the dark period in the first experiment.

Arginine and histidine are both nitrogen-rich, containing three nitrogens per molecule. Arginine is an important component of cyanophycin, a nitrogen storage molecule found in cyanobacteria (Allen et al., 1980). Arginine and/or histidine could potentially serve an analogous function in *E. huxleyi*. If cells from the first experiment had experienced nutrient stress as hypothesized, once the cells were placed in nutrient-replete media these amino acids could have been accumulated as a nitrogen store. This prospect would have caused the ninhydrin-assessed THAA levels to be higher than those detected using GC-FID at the onset of the dark period. Two thiols (arginine-cysteine and glutamine-cysteine) have been reported to increase in *E. huxleyi* strain CCMP373 (Sargasso Sea) when nitrogen-limited cells were spiked with inorganic nitrogen (Dupont et al., 2004). However, the mole percents of neither glutamine nor cysteine increased in strain 1742 during the dark period in the first experiment (table 3.4), and there are no

reports of storage proteins such as cyanophycin in *E. huxleyi*. The present supposition would require investigation. Further work is required to determine if specific amino acids can serve as a nitrogen store in *E. huxleyi*.

Conclusion

5.1 Conclusions

A five-day period of darkness was shown to affect cellular nitrogen dynamics in the first (February) experiment I conducted with *E. huxleyi* strain 1742. During the dark period, there was a significant drawdown of media nutrients, matched with an increase in particulate nitrogen (PN, table 3.3), which corroborated previous findings (Fig. 1.1). The increase in PN was attributable to an increase in amino acids (THAA; section 3.2). Measures of THAA during this period were higher using the ninhydrin method than using the GC-FID method, suggesting the possible importance of arginine, histidine, and/or tryptophan accumulation in the first experiment (section 4.5).

A loss of alkenones during darkness was found in all experiments I conducted with both strains 372 and 1742, corroborating previous findings (Figs. 1.1 and 1.2). In strain 1742, the alkenone carbon loss was not reflected in the POC values, suggesting that the alkenone carbon was not respired from the cell, but converted into some other cellular carbon fraction (section 3.5). However, the amount of carbon loss attributable to alkenones was insufficient to account for the apparent carbon gain in the form of THAA. Therefore, another carbon-containing compound, such as carbohydrates, is partially or fully responsible for the apparent increase in THAA carbon.

Though this behavior occurred during the first experiment with strain 1742, the second (May) and third (September) experiments did not demonstrate any significant increases in PN or THAA, or decreases in media nutrients. Cochlan et al. (1991) have hypothesized that both light intensity and nutrient availability affect dark-period nitrate

uptake in phytoplankton, based on field research in the Strait of Georgia, B.C. The high light intensity used in the present experiments (165 μEin/m^2s) compared with the low light intensity used previously (60 μEin/m^2s) may explain the lack of dark-period nitrogen dynamics during the second and third experiments. This circumstance may have been less important during the first experiment due to a nutrient stress inadvertently imposed on cells used to inoculate the experimental cultures.

E. huxleyi strain 372 showed no evidence of dark-period nutrient uptake or PN increases in this work (table 3.2), a finding in agreement with previous experiments with both strains 372 and 370 (Fig 1.2, Appendix A). Hence, strain 1742 appears physiologically unique in regard to its dark-period nitrogen dynamics. This uniqueness does not extend to its THAA composition, however, which did not change during the dark period as gauged by GC-FID analysis and was identical to the composition of strain 372 (Fig. 3.1).

5.2 Future Work

The disparity among the experiments with strain 1742, both in this work and previous studies (Fig. 1.1), suggest that dark-period nitrate uptake is dependant on factors not well-controlled in this work, namely light intensity and nutrient history. In the ocean, *E. huxleyi* cells have been found living near the deep chlorophyll maximum layer (DCML), which is situated at low light levels (section 4.3). Investigating the role that light and nutrient stress has on dark-period nutrient uptake and amino acid (THAA) production may enhance the understanding of how this organism reacts to and survives in its environment.

The effects of both light intensity and nutrient stress could be investigated simultaneously by running three experiments with strain 1742. Replicate experiments could be run identically to those here, but with three different light intensities: one experiment at a very low level (~10 μEin/m^2s), a second at an intensity just below light-saturation (60 μEin/m^2s), and a third at a high intensity (165 μEin/m^2s). By using light levels of 60 and 165 μEin/m^2-s in the future experiments, the work presented here could be used as a comparison. The experiments could additionally investigate nutrient stress by using two experimental flasks per light intensity. One flask would be inoculated with nutrient-stressed cells, and one with cells growing exponentially in batch culture. A comparison of the two flasks would allow an assessment of nutrient-stress effects on dark-period nitrogen dynamics. A comparison of each nutrient treatment among the three light intensities would allow a similar assessment of light intensity.

To definitively trace the path of nitrogen during these experiments, isotopic tagging could be employed. By adding a pulse of $^{15}NO_3^-$ into the media after cells enter continuous darkness and cell division stops, any nitrate taken up during the dark period could be traced to cellular components. Both PN and THAA can be measured by interfacing a mass spectrometer to an elemental analyzer (which allows PN measurement) and to a GC (which allows individual amino acid analysis), respectively. If THAA nitrogen becomes enriched during darkness, and PN experiences the same effect, this would verify dark-period protein synthesis and could evaluate whether any uptake is compound-specific.

Carbohydrates are the carbon source for dark-period protein production in other phytoplankton (section 4.1) and may be in *E. huxleyi* strain 1742 as well (section 3.5). It

becomes important that future experiments investigating dark-period protein accumulation measure carbohydrates. Definitively proving where the THAA carbon comes from would require isotopic tagging. However, placing a ^{13}C tag specifically onto either alkenones or carbohydrates would be quite challenging, and so the carbon mass balance approach used here must be relied upon. Certainly, any future continuous darkness experiments with *E. huxleyi* that examine protein production would do well to closely monitor the relationship between alkenones, carbohydrates, nutrient uptake, PN, and amino acids.

The GC-FID method allows the amino acid composition of phytoplankton to be ascertained, with the exception of arginine, histidine, and tryptophan. Future experiments with *E. huxleyi* that employ isotopic tracing would benefit from the use of the GC-FID method, as it can be paired with mass spectrometry to measure nitrogen-enrichment of THAA (Freedman et al., 1988; Silfer et al., 1991; Macko et al., 1997). High performance liquid chromatography (HPLC) can also be paired with mass spectrometry for the same purpose (Matsumoto and Tsuge, 1986). However, the advantage of using these two methods is limited; the amino acid composition of phytoplankton is similar (Cowie and Hedges, 1996) and, at least for *E. huxleyi*, does not change during darkness (Fig. 3.1). Barring the use of isotopic tracers in future experiments, the ninhydrin method would be the best method for THAA determination since it is faster and more robust. Though the ninhydrin method did underestimate GC-FID values during BSA analysis, this was probably due to the fact that recovery-correction was not employed.

In addition, though bacteria were determined not be of significance during the work here (section 4.4), use of staining/ epifluorescence methods (Noble and Fuhrman,

1998) would provide a guarantee that bacteria are not present in experimental cultures and accountable for the unusual uptake of nitrate by the single strain of *E. huxleyi*. Though this strain has been investigated with only partial success in the present work, the dark experiments have revealed a complexity in this organism that has previously gone unexamined. This thesis may serve as a springboard for future research regarding how *E. huxleyi* subsists in its environment.

Bibliography

Allen, M. M., Hutchison, F., and Weathers, P. J. (1980) Cyanophycin Granule Polypeptide Formation and Degradation in the Cyanobacterium *Aphanocapsa* 6308. *J. Bacteriol.* 141:2, 687-693.

Berry, D. A. and Lindgren, B. W. (1996) *Statistics: Theory and Methods*. Chapter 12: Comparing Two Populations and Chapter 15: Regression. Duxbury Press, pp. 487-519, 589-618.

Cochlan, W. P., Price, N. M., and Harrison, P. J. (1991) Effects of irradiance on nitrogen uptake by phytoplankton: comparison of frontal and stratified communities. *Mar. Ecol. Prog. Ser.* 69, 103-116.

Conte, M. H., D'Hondt, S., Quinn, J. G., Zhang, J., and Hargraves, P. E. (1998) An effect of dissolved nutrient concentrations on alkenone-based temperature estimates. *Paleoceanogr.* 13(2), 122-126.

Cooney, R. T. (2004) Biological and Chemical Oceanography. *Dynamics of the Gulf of Alaska* http://www.evostc.state.ak.us/gem/documents.html Chapter 6, 49-58.

Cowie, G.L. and Hedges, J. I. (1996) Digestion and alteration of the biochemical constituents of a diatom (*Thalassiosira weissflogii*) ingested by an herbivorous zooplankton (*Calanus pacificus*). *Limnol. Oceanogr.* 41(4), 581-594.

Cowie, G. L. and Hedges, J. I. (1992) Sources and reactivities of amino acids in a coastal marine environment. *Limnol. Oceanogr.* 37(4), 703-724.

Cuhel, R. L., Ortner, P. B., and Lean, D. R. S. (1984) Night synthesis of protein by algae. *Limnol. Oceanogr.* 29(4), 731-744.

Cullen, J. J. (1985) Diel vertical migration by dinoflagellates: Roles of carbohydrate metabolism and behavioral flexibility. *Contrib. Mar. Sci. (suppl)* 27, 135-152.

Cullen, J. J. and MacIntyre, J. G. (1996) *Physiological Ecology of Harmful Algal Blooms*. Behavior, Physiology and the Niche of Depth-Regulating Phytoplankton. Springer-Verlag, Berlin, pp.559-579.

Dupont, C. L, Nelson, R. K., Bashir, S., Moffett, J. W., and Ahner, B. A. (2004) Novel copper-binding and nitrogen-rich thiols produced and exuded by *Emiliania huxleyi*. *Limnol. Ocenogr.* 49(2), 1754-1762.

Engel, M. H. and Hare, P. E. (1985) *Chemistry and Biochemistry of the Amino Acids.* Gas-Liquid Chromatographic Separation of Amino Acids and their Derivatives. Chapman and Hall, London, pp. 462-479.

Epstein, B. L., D'Hondt, S., and Hargraves, P. E. (2001) The possible metabolic role of C_{37} alkenones in *Emiliania huxleyi*. *Org. Geochem.* 32, 867-875.

Epstein, G. L., D'Hondt, S., Quinn, J. G., Zhang, J., and Hargraves, P. E. (1998) An effect of dissolved nutrient concentrations on alkenone-based temperature estimates. *Paleoceanogr.* 13(2), 122-126.

Foy, R.H. and Smith, R. V. (1980) The role of carbohydrate accumulation in the growth of planktonic *Oscillatoria* species. *Br. Phycol. J.* 15, 139-150.

Frankignoulle, M., Canon, C., and Gattuso, J.-P. (1994) Marine calcification as a source of carbon dioxide: Positive feedback of increasing atmospheric CO_2. *Limnol. Oceanogr.* 39(2), 458-462.

Freedman, P. A., Gillyon, E. C. P., and Jumeau, E. J. (1988) Design and application of a new instrument for GC-Isotope ratio MS. *Am. Lab.* June, 114-119.

Green, J. C., Course, P. A., and Tarran, G. A. (1996) The life-cycle of *Emiliania huxleyi*: A brief review and a study of relative ploidy levels using flow cytometry. *J. mar. Syst.*, 9, 33-44.

Hedges, J. I., Baldock, J. A., Gélinas, Y., Lee, C., Peterson, M. L., and Wakeham, S.G. (2002) The biochemical and elemental composition of marine plankton: A NMR perspective. *Mar. Chem.* 78, 47-63.

Hedges, J. I. and Stern, J. H. (1984) Carbon and nitrogen detection of carbonate-containing solids. *Limnol. Oceanogr.* 29, 657-663.

Herbert, T. D. (2003) *Treatise on Geochemistry*. Chapter 15: Alkenone paleotemperature determinations. Elsevier, 6: 391-432.

Hirayama, K., Akashi, S., Furuya, M., and Fukuhara, K. (1990) Rapid confirmation of revision of the primary structure of bovine serum albumin by ESIMS and Frit-FAB LC/MS. *Biochem and Biophys. Res. Comm.* 173(2), 639-646.

Holligan, P. M., Fernández, E., Aiken, J., Balch, W. M. Boyd, P., Burkill, P. H., Finch, M., Groom, S. B., Malin, G., Muller, K., Purdie, D. A., Robinson, C., Trees, C. C., Turner, S. M., and VanderWal, P. (1993) Biogeochemical study of the coccolithophore Emiliania huxleyi in the North Atlantic. *Global Biogeochem. Cycles* 7(4), 879-900.

Joassin, P., Delille, B., Soetaert, A., Borges, A. V., Chou, L., Engel, A., Gattuso, J.-P., Harlay, J., Riebesell, U., Suykens, K., and Gregoire, M. (2008) A mathematical modeling of bloom of the coccolithophore Emiliania huxleyi in a mesocosm experiment. *Biogeosci. Discuss.* 5, 787-840.

Karl, D. M., Bidigare, R. R., and Letelier, R. M. (2002) *Phytoplankton productivity: carbon assimilation in marine and freshwater.* Sustained interannual variability of phytoplankton processes: Pacific Subtropical Gyre. Blackwell Science, Oxford, pp. 222–264.

Lehninger, A. L. (1975) Biochemistry. Worth Publishers, New York, New York, p. 70.

Lindberg, V. (2000) Uncertainties and Error Propogation. *Uncertainties, Graphing, and the Vernier Caliper, Part I.*
www.rit.edu/cos/uphysics/uncertainties/Uncertaintiespart2.html

Lipschultz, F., Bates, N. R., Carlson, C. A., and Hansell, D. A. (2002) New production in the Sargasso Sea: History and current status. *Global Biogeochem. Cycles.* 16(1), 10.1029.

Macko, S.A., Uhle, M. E., Engel, M. H., and Andrusevich, V. (1997) Stable nitrogen isotope analysis of amino acid enantiomers by gas chromatography/combustion/isotope ratio mass spectrometry. *Anal. Chem.* 69, 926-929.

Marlowe, I. T., Green, J.C., Neal, A.C., Brassell, S.C., Eglinton, G., and Course, P.A. (1984) Long chain alkenones in the Prymnesiophyceae. Distribution of alkenones and other lipids and their taxonomic significance. *Br. phycol. J.* 19, 251-255.

Matsumoto, K. and Tsuge, S. (1986) Analysis of Free- and PTH-Amino Acids by HPLC-MS with Self-Spouting and Vacuum Nebulizing Assisted Interface. *Mass Spectrosc.* 34:4, 243-248.

Moore, S. (1968) Amino acid analysis: aqueous dimethyl sulfoxide as solvent for the ninhydrin reaction. *J. Biol. Chem.* 243:23, 6281-6283.

Muggli, D. L. and Harrison, P. J. (1996) Effects of nitrogen source on the physiology and metal nutrition of *Emiliania huxleyi* grown under different iron and light conditions. *Mar. Ecol. Prog. Ser.* 130, 255-267.

Muller, P. J., Kirst, G., Ruhland, G., von Storch, I., and Rosell-Mele, A. (1998) Calibration of the alkenone paleotemperature index $U_{37}^{K'}$ based on core-tops from the eastern South Atlantic and the global ocean (60^{o}N-60^{o}S). *Geochim. Cosmochim. Acta* 62, 1757-1772.

Nagata, T. (1986) Carbon and nitrogen content of natural planktonic bacteria. *App. Environ. Microbiol.* 52(1), 28-32.

Noble, R. T. and Fuhrman J. A. (1998) Use of SYBR Green I for rapid epifluorescence counts of marine viruses and bacteria. *Aquat. Microb. Ecol.* 14, 113-118.

Ohkouchi, N, Kawamura, K., Kawahata, H., and Okada, H. (1999) Depth ranges of alkenone production in the central Pacific Ocean. *Global Biogeochem. Cycles* 13(2), 695-704.

Okada, H., and Honjo, S., (1973) The distribution of oceanic coccolithophorids in the Pacific. *Deep-Sea Res. Part A* 20, 355-374.

Paasche, E., Bryceson, I., and Tangen, K. (1984) Interspecific variation in dark nitrogen uptake by dinoflagellates. *J. Phycol.* 20, 394-401.

Prahl, F. G., Collier, R. B., Dymond, J., Lyle, M., and Sparrow, M. A. (1993) A biomarker perspective on prymnesiophyte productivity in the northeast Pacific Ocean. *Deep-Sea Res.* 40(10), 2061-2076.

Prahl, F. G., Muelhausen, L. A., and Zahnle, D. L. (1988) Further evaluation of long-chain alkenones as indicators of paleoceanographic conditions. *Geochim. et Cosmochim. Acta* 52, 2303-2310.

Prahl, F. G., Popp, B. N., Karl, D. M., and Sparrow, M. A. (2005a) Ecology and biogeochemistry of alkenone production at station ALOHA. *Deep-Sea Res. I, in press*.

Prahl, F.G., Rontani, J., Volkman, J.K., Sparrow, M.A., Royer, I.M. (2005b) 'Unusual' C_{35} and C_{36} alkenones in a paleoceanographic benchmark strain of *Emiliania huxleyi*. *Geochim. et Costmochim Acta.* In press.

Prahl, F. G., Wolfe, G. V., and Sparrow, M. A. (2003) Physiological impacts on alkenone paleothermometry. *Paleoceanogr.* 18(2), 1025.

Richardson, T. L., Ciotti, Á. M., Cullen, J. J., and Villareal, T. A. (1996) Physiological and optical properties of *Rhizosolenia Formosa* (Bacillariophyceae) in the context of open-ocean vertical migration. *J. Phycol.* 32, 741-757.

Richardson, T. L. and Cullen, J.J. (1995) Changes in buoyancy and chemical composition during growth of a coastal marine diatom: ecological and biogeochemical consequences. *Mar. Ecol. Prog. Ser.* 128, 77-90.

Schafer, H., Abbas, B., Witte, H., and Muyzer, G. (2002) Genetic diversity of 'satellite' bacteria present in cultures of marine diatoms. *FEMS Microbiology Ecol.* 42, 25-35.

Silfer, J. A., Engel, M. H., Macko, S. A., and Jumeau, E. J. (1991) Stable carbon isotope analysis of amino acid enantiomers by conventional isotope ratio mass spectrometry and

combined gas chromatography/isotope ratio mass spectrometry. *Anal. Chem.* 63, 370-374.

Strickland, J. D. H. and Parsons, T. R. (1972) *A Practical Handbook of Seawater Analysis, 2nd ed.,* Bull. Fish. Res. Board Can. 167: 310pp.

Styrett, P. J. (1981) *Physiological Bases of Phytoplankton Ecology*. Nitrogen metabolism of microalgae. Canadian bulletin of fisheries and aquatic sciences. Ottowa, Canada, 210: 182-210.

Vallina, Sergio M. and Simó, Rafel (2007). Strong Relationship Between DMS and the Solar Radiation Dose over the Global Surface Ocean. Science 315(5811), 506-508.

Van Rijn, J., and Shilo, M. (1985). Carbohydrate fluctuations, gas vacuolation, and vertical migration of scum-forming cyanobacteria in fishponds. *Limnol. Oceanogr.* 30, 1219-1228.

Verardo, D. J., Froelich, P. N., and McIntyre, A. (1990) Determination of organic carbon and nitrogen in marine sediments using the Carlo Erba NA-1500 Analyzer. *Deep-Sea Res.* 37(1), 157-165.

Villareal, T. A., and Carpenter, E. J. (2002) Buoyancy regulation and the potential for vertical migration in the oceanic cyanobacterium *Trichodesmium*. *Microb. Ecol.* 10.1007

Villareal, T. A., Joseph, L., Brzezinski, M. A., Shipe, R. F., Lipschultz, F., and Altabet, M. A. (1999) Biological and chemical characteristics of the giant diatom *Ethmodiscus* (Bacillariophyceae) in the central North Pacific gyre. *J. Phycol.* 35, 896-902.

Young, J. R. (1994) *Coccolithophores*. Functions of Coccoliths. Cambridge University Press, Cambridge, pp.63-82.

Appendices

Appendix A: Data for previous continuous darkness experiments with *E. huxleyi* strains 1742 and 372 (Prahl and coworkers, unpublished data), used in figures 1.2 and 1.3. Data is listed as pg/cell unless otherwise noted. Alkenone carbon data assumes a value of 80% carbon by weight. Experiment conditions: 60 µEin/m2s, ~15oC, f/20 media

							µM						
Strain	Light/Dark	Date	Cells/mL (E+5)	POC	PN	ΣAlk	ΣAlk C	POC	PN	NO3	NO2	PO4	C/N (at)
1742	Lt	11/15/2001	2.04	6.31	0.71	1.60	67	108	10	82	0.19	11.4	10.4
1742	Lt	11/16/2001	3.06	6.67	0.75	1.53	67	168	16	74	0.34	10.8	10.2
1742	Dk	11/17/2001	3.82	4.60	0.60	1.32	40	147	16	71	0.44	10.5	9.0
1742	Dk	11/18/2001	4.00	4.43	0.63	1.01	30	148	18	70	0.40	10.4	8.2
1742	Dk	11/19/2001	4.17	4.36	0.72	0.62	18	152	21	65	0.42	10.2	7.1
1742	Dk	11/20/2001	4.02	4.95	0.86	0.50	16	166	25	60	0.47	9.8	6.7
1742	Dk	11/21/2001	3.99	5.16	1.04	0.46	16	172	30	52	0.55	9.3	5.8
1742	Lt	11/22/2001	3.99	6.53	1.09	0.75	33	218	31	44	0.64	9.1	7.0
1742	Lt	11/23/2001	3.91	11.43	2.03	1.15	87	373	57	28	0.80	8.3	6.6
1742	Lt	11/24/2001	5.61	11.27	1.94	1.39	104	527	78	6	1.20	7.0	6.8
1742	Lt	11/25/2001	6.50	12.35	1.82	1.77	146	669	84	0	0.45	5.5	7.9
372	Lt	10/18/2002	0.65	11.48	1.32	1.36	104	62	6	80	0.03	3.9	10.1
372	Lt	10/19/2002	0.94	10.50	1.19	1.35	94	83	8	80	0.08	3.7	10.3
372	Lt	10/20/2002	1.40	10.00	1.10	1.36	91	117	11	76	0.22	3.4	10.6
372	Lt	10/21/2002	1.70	11.31	1.51	1.42	107	160	18	71	0.22	3.2	8.7
372	Dk	10/22/2002	2.99	5.71	0.81	0.65	25	143	17	69	0.16	2.8	8.2
372	Dk	10/23/2002	3.00	5.67	0.98	0.50	19	142	21	70	0.11	2.8	6.8
372	Dk	10/24/2002	2.94	5.64	0.88	0.50	19	138	19	68	0.25	2.7	7.5
372	Dk	10/25/2002	3.60	4.73	0.73	0.36	11	142	19	71	0.37	2.9	7.5
372	Dk	10/26/2002	2.88	5.59	0.86	0.53	20	134	18	68	0.39	2.6	7.6
372	Lt	10/27/2002	3.06	12.34	1.98	1.17	97	314	43	60	0.50	2.0	7.3
372	Lt	10/28/2002	8.71	6.06	0.76	0.83	34	440	47	40	0.59	0.9	9.3
372	Lt	10/29/2002	13.57	5.96	0.76	0.86	34	674	74	10	0.46	0.1	9.2

Appendix A (continued)

							µM						
Strain	Light/Dark	Date	Cells/mL (E+5)	POC	PN	ΣAlk	ΣAlk C	POC	PN	NO3	NO2	PO4	C/N (at)
370	Lt	9/11/2002	1.81	5.98	0.75	0.45	5	90	10	85	0.13	8.5	9.3
370	Lt	9/12/2002	3.23	4.67	0.75	0.47	10	126	17	76	0.18	7.8	7.3
370	Lt	9/13/2002	5.64	4.43	0.73	0.44	17	208	30	63	0.33	6.9	7.1
370	Dk	9/14/2002	6.88	3.13	0.60	0.18	8	179	30	63	0.22	6.9	6.1
370	Dk	9/15/2002	7.03	2.99	0.58	0.12	6	175	29	63	0.21	7.0	6.0
370	Dk	9/16/2002	7.16	2.96	0.56	0.17	8	177	29	64	0.41	6.7	6.1
370	Dk	9/17/2002	7.04	3.56	0.58	0.15	7	209	29	64	0.44	7.0	7.2
370	Dk	9/18/2002	7.00	2.66	0.53	0.22	10	155	27	64	0.45	6.9	5.8
370	Lt	9/19/2002	7.00	5.73	0.78	0.87	41	334	39	55	0.49	5.9	8.6
370	Lt	9/20/2002	10.72	6.42	0.89	1.24	89	573	68	20	0.50	3.7	8.4
370	Lt	9/21/2002	23.70	4.57	0.52	1.11	175	902	89	0	0.10	0.7	10.2

Appendix B: GC amino acid data (E-06 nmol/cell) for all experiments. Days are since innoculation. Shaded regions are During continuous darkness. Days followed by a, b, and c are replicates; table 3.3 lists their average.
--- Value below minimum detection limit. No data available.

Strain 1742

Feb

Day	cells/mL (E+5)	Cys	Ala	Gly	Thr	Ser	Val	Leu	Iso	Pro	Asp	Met	Glu	Phe	Lys	Tyr	TotAA
9	2.5	---	4.57	1.94	0.83	1.76	0.70	1.87	0.00	1.59	2.32	0.75	3.35	1.17	1.62	0.30	23
10	3.2	---	3.73	2.47	1.12	1.83	0.87	2.39	0.48	1.70	2.37	0.51	3.64	1.46	1.70	0.52	25
11*	3.1	---	3.51	2.94	1.43	2.18	1.07	2.95	0.63	1.92	3.48	0.40	5.23	1.99	1.91	0.43	30
12	3.4	---	4.81	3.55	1.39	2.48	0.92	2.96	0.49	2.24	3.54	---	6.10	1.96	2.52	0.79	34
13	3.5	---	5.72	4.12	1.74	2.22	1.28	3.49	0.65	2.66	4.42	---	7.27	2.29	2.49	0.56	39
14**	3.5																
15	5.0	---	4.52	2.89	1.48	1.98	1.34	2.61	0.76	1.92	3.58	---	5.64	1.63	1.98	0.46	31
16	4.0	---	3.95	4.48	1.05	2.00	1.74	4.59	1.27	3.78	6.91	---	10.70	3.07	3.72	0.24	48

* Sample went unfrozen for 24 hours after collection.

** Low hydrolysis volume. Sample rejected.

May

Day	cells/mL (E+5)	Cys	Ala	Gly	Thr	Ser	Val	Leu	Iso	Pro	Asp	Met	Glu	Phe	Lys	Tyr	TotAA
17	2.6	0.69	2.24	2.09	0.96	0.95	1.25	1.85	0.91	1.20	2.11	---	2.65	0.94	1.63	0.10	20
18	2.4	0.61	3.15	2.90	1.69	1.41	1.65	2.68	1.19	1.57	2.86	---	3.56	1.21	1.48	0.45	26
19	2.3	0.38	3.26	3.28	0.72	---	2.13	3.05	1.57	1.77	3.21	---	4.06	1.46	1.91	0.29	27
20	2.3	0.47	1.90	2.87	1.11	---	1.17	2.92	1.06	2.28	4.09	---	4.81	1.70	2.29	0.21	27
21	2.6	0.58	2.13	2.95	1.43	---	1.57	2.98	1.35	1.88	3.63	---	4.14	1.65	2.04	0.26	27
22	2.5	0.21	3.70	3.61	1.01	---	1.99	2.98	1.37	1.75	3.47	---	4.17	1.59	1.56	0.69	28
23	2.7	1.45	2.30	3.65	2.07	3.41	1.92	4.17	2.02	2.69	5.98	1.09	7.33	2.59	3.30	2.63	45

Appendix B (continued)

Sept

Day	cells/mL (E+5)	Cys	Ala	Gly	Thr	Ser	Val	Leu	Iso	Pro	Asp	Met	Glu	Phe	Lys	Tyr	TotAA
9	1.8	1.02	3.49	3.38	1.32	1.00	1.42	2.78	0.94	1.73	3.11	---	3.62	1.10	0.78	0.61	26
10	3.5	0.45	2.31	2.42	0.42	0.65	1.36	2.66	1.07	1.66	2.90	---	3.33	1.23	1.31	0.36	22
11	4.0	0.30	2.16	2.05	0.48	0.64	0.95	1.97	0.66	1.30	2.28	---	2.74	0.86	1.18	0.53	18
12	3.9	0.61	2.59	2.61	0.32	0.79	1.28	2.36	0.92	1.52	2.64	---	2.98	1.10	1.24	0.46	21
13	4.2	0.42	2.61	2.76	0.27	0.72	1.37	2.44	0.97	1.52	2.72	---	3.13	1.10	1.07	0.36	21
14a	3.9	0.80	3.15	3.01	0.96	1.30	1.30	2.74	0.96	1.83	3.24	---	3.78	1.33	1.09	0.64	26
14b	3.9	0.53	3.06	2.66	0.38	0.99	1.49	2.44	1.05	1.57	2.65	---	3.07	1.14	1.34	0.54	23
14c	3.9	0.43	2.71	2.41	0.90	1.46	1.10	2.37	0.95	1.56	2.79	---	3.23	1.12	0.86	0.56	22
15	4.3	0.26	2.34	2.79	1.06	1.72	1.12	2.61	0.82	1.88	3.11	---	3.57	1.21	1.00	0.45	24
16	5.1	0.45	2.69	2.61	1.34	1.77	1.36	2.65	1.02	1.59	2.96	---	3.64	1.22	1.43	0.62	25
17	6.5	0.32	3.17	3.02	1.36	1.76	1.62	3.14	1.18	1.90	3.47	---	4.67	1.47	2.21	0.81	29

Strain 372

May

Day	cells/mL (E+5)	Cys	Ala	Gly	Thr	Ser	Val	Leu	Iso	Pro	Asp	Met	Glu	Phe	Lys	Tyr	TotAA
18	2.6	1.83	2.69	4.23	1.10	---	1.87	5.12	1.86	3.62	7.49	---	8.88	3.53	3.16	0.91	46
19	2.6	1.22	3.67	3.68	1.10	---	2.77	4.31	2.20	2.52	4.41	---	4.55	2.03	1.84	0.55	35
20	2.2	1.55	4.28	4.10	2.16	2.90	2.32	4.23	1.84	2.50	4.85	0.29	4.90	1.97	1.64	1.84	41
21	2.5	0.93	3.85	3.67	1.32	2.07	1.73	3.36	1.20	2.05	4.00	---	3.94	1.58	1.42	0.78	32
22	2.5	0.59	3.53	3.70	1.56	2.94	2.08	3.84	1.71	2.34	4.83	---	5.13	1.98	2.00	2.28	39
23	3.1	1.95	3.59	4.11	0.80	0.96	1.90	3.87	1.33	2.47	4.76	0.29	5.32	1.80	1.60	0.24	35
24	10.2	0.41	2.70	2.28	1.34	1.71	1.86	2.46	1.34	1.36	2.71	0.10	3.20	1.01	1.20	0.63	24

Appendix B (continued)

Sept

Day	cells/mL (E+5)	Cys	Ala	Gly	Thr	Ser	Val	Leu	Iso	Pro	Asp	Met	Glu	Phe	Lys	Tyr	TotAA
7	3.9	0.69	1.09	1.69	0.76	1.86	0.76	2.29	0.64	1.69	2.99	---	3.95	1.29	1.31	0.99	22
8	5.7	1.05	2.91	2.48	1.42	1.51	1.14	2.70	1.01	2.05	2.43	1.10	3.38	1.22	0.98	1.02	26
9	5.4	0.45	2.08	2.24	0.97	1.64	1.06	2.62	0.82	1.67	2.86	---	3.22	1.22	1.26	0.67	26
10a	5.7	0.48	2.88	2.45	0.95	1.53	0.99	2.19	0.64	1.40	2.30	---	2.61	0.96	1.03	0.68	20
10b	5.7	0.74	1.48	2.17	0.46	1.04	0.67	2.33	0.50	1.64	2.80	---	3.13	1.16	1.22	0.36	19
10c	5.7	0.31	2.05	2.40	0.59	0.93	0.82	2.33	0.60	1.65	2.79	---	3.30	1.13	1.35	0.36	20
11*	5.5																
12	5.7	0.53	1.86	2.03	1.04	1.89	1.08	2.39	0.88	1.54	2.76	---	2.92	1.12	1.15	1.27	22
13**	7.7																
14	10.3	0.37	3.12	3.28	0.82	0.57	1.59	3.10	1.12	2.01	3.26	---	3.86	1.31	1.55	0.07	26

*Suspicious value, cause unknown. Rejected.

** No sample.

Appendix C: Alkenone data (E-02 pg/cell) for all experiments. Shaded regions are during continuous darkness. Days are since innoculation. gT is the growth temperature calculated using Uk'37 and the calibration equation Uk'37 = 0.034*T + 0.039 (Prahl et al., 1988).

Strain 1742

Feb

Day	cells/mL (E+05)	cK37:4m	cK37:3m	cK37:2m	cK38:3e	cK38:3m	cK38:2e	cK38:2m	cK39:3e	cK39:2e	K35/K36	K35/K37	ΣAlk	Uk'37	gT
9	2.5	1.0	31.6	37.3	9.3	8.9	16.7	8.3	1.2	0.2	---	---	115	0.54	14.8
10	3.2	1.0	28.4	29.3	8.4	7.9	14.1	6.7	1.0	2.1	---	---	99	0.51	13.8
11*	3.1	0.1	4.6	5.7	2.3	1.5	4.1	1.6	0.5	0.5					15.1
12	3.4	0.4	14.3	16.0	6.9	5.0	10.6	4.2	0.9	1.4	---	---	60	0.53	14.4
13	3.5	0.1	7.1	9.0	4.8	3.0	7.3	2.8	0.6	1.2	---	---	36	0.56	15.3
14	3.5	0.1	5.9	8.3	5.3	2.7	7.7	2.7	0.8	1.1	---	---	35	0.58	16.0
15	5.0	0.2	9.2	14.5	5.2	3.8	9.3	4.6	0.7	1.6	---	---	49	0.61	16.9
16	4.0	0.6	28.4	39.0	12.4	9.7	22.3	10.8	1.7	3.2	---	---	128	0.58	15.9

* Sample went unfrozen for 24 hours after collection. Value rejected.

--- Below detection limit. No data available.

May

Day	cells/mL (E+05)	cK37:4m	cK37:3m	cK37:2m	cK38:3e	cK38:3m	cK38:2e	cK38:2m	cK39:3e	cK39:2e	K35/K36	K35/K37	ΣAlk	Uk'37	gT
16	1.5	1.0	29.6	0.3	21.7	3.0	11.0	10.7	13.0	5.9	3.6	2.6	102	0.42	11.3
17	2.6	0.6	17.0	0.1	13.1	2.0	6.2	5.7	7.5	3.2	1.6	1.2	58	0.43	11.6
18	2.4	1.7	44.9	0.5	30.7	5.3	17.2	15.6	18.9	8.0	3.1	3.1	149	0.41	10.8
19	2.3	0.7	25.6	0.3	18.4	3.9	12.1	9.9	13.2	5.1	2.2	2.5	94	0.42	11.2
20	2.3	0.5	22.4	0.2	17.5	4.6	13.4	9.8	14.2	5.6	2.5	2.5	93	0.44	11.8
21	2.6	0.2	9.5	0.1	7.8	2.4	6.9	4.7	7.4	2.7	1.7	1.5	45	0.45	12.2
22	2.5	0.4	17.7	0.1	14.5	4.7	15.0	9.3	16.2	5.1	3.5	3.3	90	0.45	12.1
23	2.7	0.6	31.4	0.3	32.0	5.4	17.6	13.7	22.3	10.2	3.6	4.6	142	0.50	13.7
24	5.6	0.6	34.4	0.2	32.5	5.1	14.1	13.0	18.0	9.3	5.0	3.1	135	0.49	13.2

Appendix C (continued)

Strain 372

May

Day	cells/mL (E+05)	cK37:4m	cK37:3m	cK37:2m	cK38:3e	cK38:3m	cK38:2e	cK38:2m	cK39:3e	cK39:2e	K35/K36	K35/K37	ΣAlk	UK'37	gT
16	2.0	0.2	13.9	1.5	3.7	2.7	4.4	4.9	1.6	1.0	1.1	0.3	35	0.21	5.0
17	2.5	0.2	30.6	3.8	6.6	6.1	9.4	10.2	2.9	1.8	1.8	0.6	74	0.18	4.0
18	2.5	0.0	15.7	2.8	3.6	4.4	7.0	6.7	2.1	1.3	1.8	0.3	46	0.19	4.3
19	2.6	0.0	14.4	2.2	3.7	4.9	8.1	7.0	2.5	1.4	1.5	0.4	46	0.20	4.8
20	2.2	0.0	11.9	2.0	3.2	5.1	8.4	6.7	2.7	1.4	1.6	0.4	43	0.21	5.1
21	2.5	0.0	4.0	1.0	0.9	2.2	3.6	2.5	0.9	0.5	0.8	0.2	17	0.19	4.3
22	2.5	0.0	6.9	1.3	1.9	4.1	6.9	4.6	2.1	1.0	1.3	0.5	31	0.22	5.3
23	3.1	0.0	32.6	2.6	9.8	5.1	11.1	12.4	4.3	2.6	2.3	0.7	83	0.23	5.7
24	11.1	0.0	18.4	1.3	4.5	2.7	4.6	5.6	1.5	1.0	0.9	0.2	41	0.20	4.6

--- Below detection limit. No data available.